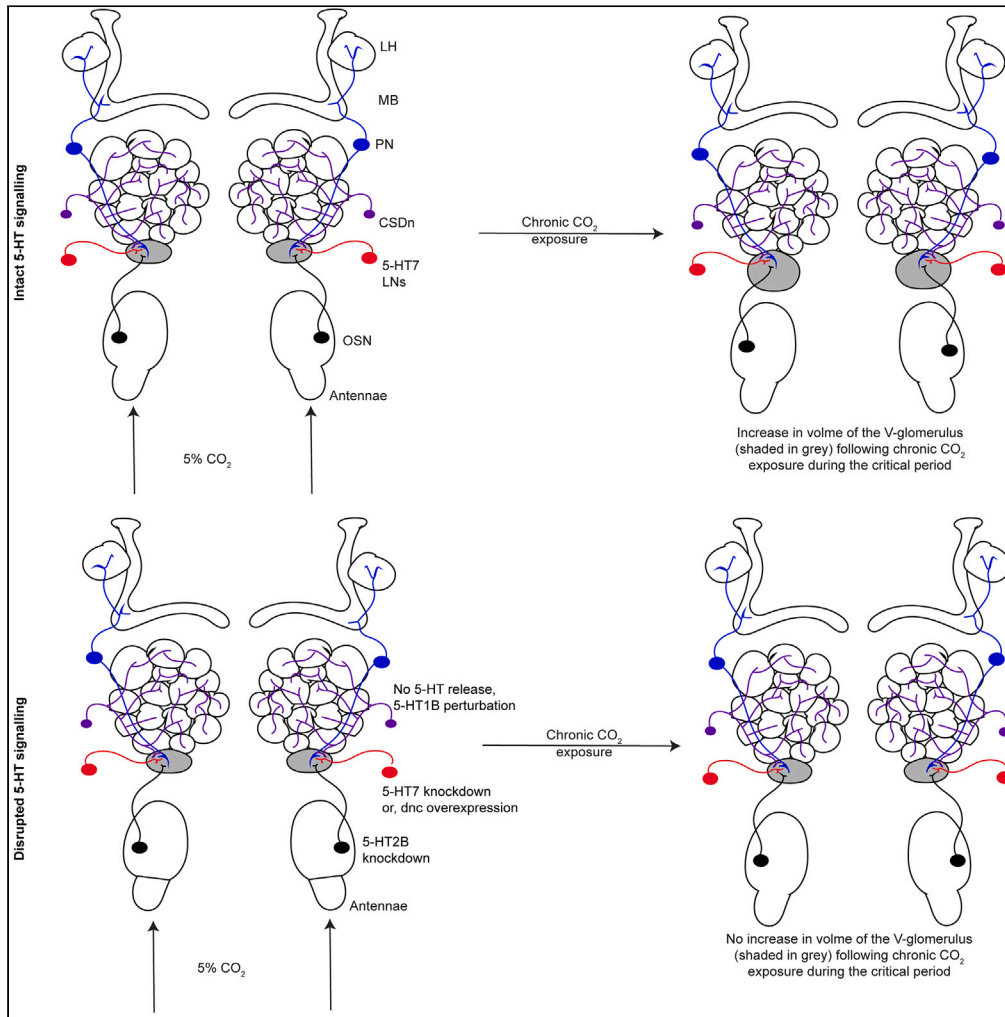


Article

Serotonin acts through multiple cellular targets during an olfactory critical period



Ahana Mallick, Hua Leonhard Tan (譚華), Jacob Michael Epstein, Clarissa Mei Jing Ng, Oliver Mason Cook, Quentin Gaudry, Andrew M. Dacks

amd358@case.edu

Highlights

5-HT modulates structural plasticity via multiple 5-HTRs

5-HT modulates both excitatory (OSNs) and inhibitory (LNs) components of olfaction

SSRI treatment induces critical period like structural plasticity in adults

Mallick et al., iScience 27, 111083
November 15, 2024 © 2024 The Author(s). Published by Elsevier Inc.
<https://doi.org/10.1016/j.isci.2024.111083>



Article

Serotonin acts through multiple cellular targets during an olfactory critical period

Ahana Mallick,¹ Hua Leonhard Tan (譚華),¹ Jacob Michael Epstein,¹ Clarissa Mei Jing Ng,¹ Oliver Mason Cook,² Quentin Gaudry,^{1,4,5} and Andrew M. Dacks^{2,3,4,5,6,*}

SUMMARY

Serotonin (5-HT) modulates early development during critical periods when experience drives heightened levels of plasticity in neurons. Here, we investigate the cellular mechanisms by which 5-HT modulates critical period plasticity (CPP) in the olfactory system of *Drosophila*. We first demonstrate that 5-HT is necessary for experience-dependent structural plasticity in response to chronic CO₂ exposure and can re-open the critical period long after it normally closes. Knocking down 5-HT₇ receptors in a subset of GABAergic local interneurons was sufficient to block CPP, as was knocking down GABA receptors expressed by CO₂-sensing olfactory sensory neurons (OSNs). Furthermore, direct modulation of OSNs via 5-HT_{2B} receptors in CO₂-sensing OSNs and autoreceptor expression by serotonergic neurons was also required for CPP. Thus, 5-HT targets individual neuron types in the olfactory system via distinct receptors to enable sensory driven plasticity.

INTRODUCTION

In early postnatal life of animals, all sensory systems exhibit heightened levels of plasticity and circuit refinement in response to environmental stimuli in a specific time window called critical period. Critical period plasticity (CPP) provides an excellent readout to assess how sensory experiences shape circuits early in life at the cellular and molecular level.^{1–3} Along with sensory experiences, neuromodulators like 5-HT also play an important role in shaping CPP. Initial experiments indicating the role of 5-HT in modulating sensory critical periods was observed in both the visual and somatosensory cortices in kittens and rats.^{4–7} Similarly, 5-HT has also been shown to modulate the early postnatal development of limbic circuits such as the pre-frontal cortex in humans as well as non-human primates and rodent models. Disruption in serotonergic signaling in this circuit has been linked to an increased risk for behavioral and cognitive deficits in adult mice.^{8–11} Thus, 5-HT targets multiple effector regions during early development to facilitate proper brain development and function in adults. However, 5-HT can activate several receptor subtypes expressed by distinct cell types within a network, so the cellular mechanisms by which 5-HT impacts CPP can be difficult to identify.

We took advantage of the wealth of transgenic tools and foundational work in the olfactory system of *Drosophila* to determine how 5-HT can impact different circuit mechanisms within an olfactory critical period. The organization of the fruit fly olfactory network is similar to that in mammals^{1,12} in that olfactory processing begins upon odor binding chemoreceptive proteins localized at the dendrites of olfactory sensory neurons (OSNs).^{13–16} All OSNs expressing the same complement of chemoreceptive proteins project to a distinct glomerulus to form an olfactory map within the primary olfactory center, the antennal lobe (AL).¹⁷ OSNs synapse upon second-order projection neurons (PNs) that project onto higher order olfactory centers. The cellular and molecular mechanisms of structural plasticity observed in olfactory CPP in the fruit fly is well known.^{18–27} Similar forms of experience-dependent olfactory plasticity have also been studied extensively and reviewed in other insects like honeybees, moths, butterflies, locusts, and ants.¹⁸ Most CPP studies in *Drosophila* were conducted using either CO₂ or ethyl butyrate exposure as sensory stimuli or both. With either of the odors, chronic exposure during the critical period induced structural plasticity in the relevant glomerulus, causing a change of either an increase or a decrease in the glomerular volume. At the circuit level, the structural plasticity resulting in an increase in glomerular volume is manifested through an increase in the number of local interneuron (LN) and PN arbors innervating the glomerulus, whereas the total number of neurons remains intact.^{19–21,27} Glomerular volume decrease, on the other hand, is caused by retraction of the OSN axon fibers upon chronic ethyl butyrate exposure in a specific glomerulus.²³ These studies demonstrated that the olfactory CPP in *Drosophila* shares many of the same molecular mechanisms as visual CPPs.^{2,3,20–23,27–30} In both cases, CPP involves GABAergic and glutamatergic signaling, Ca²⁺/Calmodulin-dependent adenylate cyclase and cAMP-response element binding protein (CREB)-dependent gene transcription.^{20,21,31} However, although 5-HT neuromodulation has been shown to be required for visual critical periods in mammals,^{5–7,32–35} it has not been studied with respect to CPP in the olfactory system of mammals or insects.

¹Department of Biology, University of Maryland, College Park, MD 20742, USA

²Departments of Biology and Neuroscience, West Virginia University, Morgantown, WV 26505, USA

³Department of Biology, Case Western Reserve University, Cleveland, OH 44106, USA

⁴Senior author

⁵These authors contributed equally

⁶Lead contact

*Correspondence: amd358@case.edu

<https://doi.org/10.1016/j.isci.2024.111083>



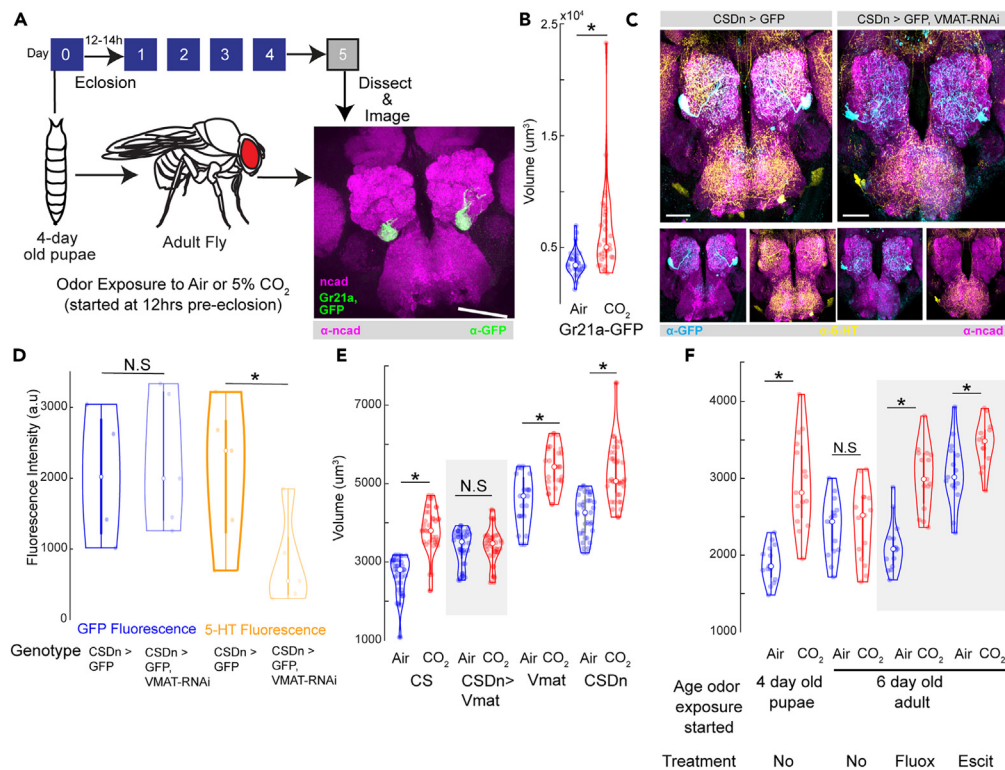


Figure 1. Blocking serotonin release from CSDNs prevents structural plasticity during the critical period

(A) Schematic of the experimental protocol. Four-day-old pupae are collected and subject to 5% CO₂ for 5 days. On day 5 after eclosion, flies are collected and stained with n-cadherin and imaged under a confocal microscope to analyze structural plasticity. Confocal maximum intensity projection of AL by CO₂-responsive V-glomerulus in green co-labeled for n-cadherin (magenta).

(B) Quantification of V-glomerulus volumes comparing air- (right) and 5% CO₂ (left)-exposed flies during the critical period. Genotype shown here is endogenously expressed GFP under the Gr21a promoter (Gr21aGFP).

(C) Confocal maximum intensity projections of AL innervation by CSDNs in CSDn-Gal4 > UAS-mcd8::GFP and CSDn-Gal4 > UAS-GFP, UAS-Vmat-RNAi flies, labeled for GFP (blue), 5-HT (yellow), and n-cadherin (magenta).

(D) Quantification of GFP (n = 4 for each genotype) and 5-HT (n = 5 for each genotype) immunofluorescence in CSDNs in CSDn-Gal4 > UAS-mcd8::GFP and CSDn-Gal4 > UAS-GFP, UAS-Vmat-RNAi flies.

(E) Quantification of V glomerulus volumes comparing air- and 5% CO₂-exposed flies during the critical period. Four genotypes are shown here from left to right: Canton-S (wildtype), CSDn-Gal4>UAS-Vmat-RNAi (CSDn targeted Vmat knockdown), w1118;UAS-Vmat-RNAi (background control for Gal4) and y,v; CSDn-Gal4 > RNAi background (background control for RNAi).

(F) Quantification of V glomerulus volumes comparing air- and 5% CO₂-exposed Canton-S flies of various ages and SSRI treatment conditions. Different experimental conditions and ages of flies are shown here from left to right: 4-day-old Canton-S pupae without SSRI, 6-day-old Canton-S flies without SSRI treatment, 6-day-old Canton-S flies with fluoxetine treatment, 6-Day-old Canton-S flies with escitalopram treatment. * indicates p < 0.05; N.S indicates p > 0.05; n ≥ 15. All violin plots include individual data points (colored circles) and mean (white circle). The boxplot of the data is also represented at the center of the violin. The scale bar indicates 50 µm, and gray boxes indicate experimental fly lines in all cases. Detailed genotypes of flies for each experimental condition can be found in Table 1 and the antibody concentrations used in Table 2.

In this study, we investigate how 5-HT modulates olfactory critical periods, and we focus on the behaviorally relevant^{36,37} CO₂-sensing circuit in *Drosophila*. Since the V glomerulus is exclusively dedicated to respond to CO₂, and the CPP mechanisms are already known for this glomerulus, it is ideal for studying the effect of serotonergic modulation. We performed cell-type specific genetic manipulations of the serotonergic system to identify where 5-HT is required during odor-evoked structural plasticity in the olfactory circuit. Our results show that during the critical period, 5-HT modulates distinct cell types in the AL via activation of different 5-HT receptor subtypes. We thus identified cell types where serotonergic modulation may be interacting with the previously described mechanisms of CPP to modulate structural plasticity during CPs.

RESULTS

Olfactory CPP requires the release of 5-HT by the serotonergic neurons

In *Drosophila*, the olfactory CPP manifests as a change in the volume of the glomerulus innervated by OSNs responsive to the odor used as a stimulus (Figures 1A and 1B).^{20,21,27} Consistent with previous reports,^{20,21,27} in flies where 5-HT transmission is intact, the V-glomerulus increased in volume in flies exposed to CO₂ compared to air exposed (Figure 1B). In *Drosophila* and other holometabolous insects, a single

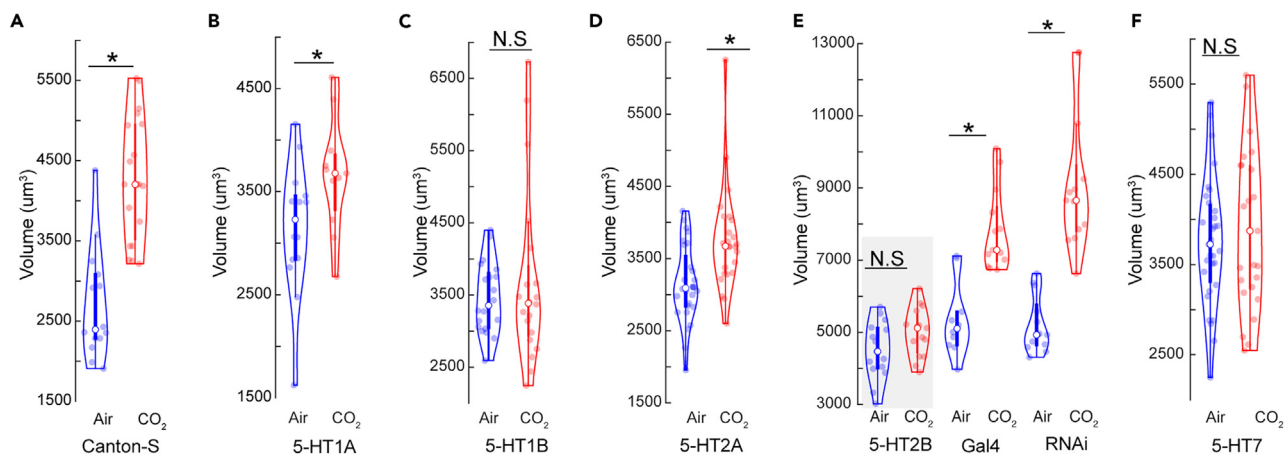


Figure 2. Serotonin acts through multiple receptors during the critical period

(A) Comparison of V-glomerulus volumes in air- and 5% CO₂-exposed brains in wild-type Canton-S flies. (B–D and F) Comparison of V-glomerulus volumes in air- and 5% CO₂-exposed brains of 5-HT1AR (B), 5-HT1BR (C), 5-HT2AR (D), and 5-HT7R (F) knockout flies. (E) Comparison of V-glomerulus volumes in air- and 5% CO₂-exposed brains of flies with genotypes (left to right): 5-HT2B knockdown in 5-HT2B heterozygous mutants, UAS-5HT2B-RNAi in Gal4 knock in background, heterozygous 5-HT2B mutant with Gal4 knock in RNAi background (*y,v; 5HT2B[Gal4] > TRiP* background). * indicates $p < 0.05$; N.S indicates $p > 0.05$; $n \geq 15$ and gray boxes indicate experimental fly lines in all cases. All violin plots include individual data points (colored circles) and mean (white circle). The boxplot of the data is also represented at the center of the violin. Detailed genotypes of the flies used in each experimental condition can be found in Table 1 and the antibody concentrations used in Table 2.

pair of serotonergic neurons called the contralaterally projecting serotonin immunoreactive deutocerebral neurons (CSDNs) innervate the AL^{38–40} (Figure 1C) and supply serotonin.^{38,40–42} We thus assessed the role of 5-HT in CPP in the *Drosophila* olfactory system by measuring the structural plasticity induced in the CO₂-sensitive V-glomerulus upon chronic exposure to 5% CO₂.^{20,21,27} We employed the R60F02-Gal4 promoter line that labels the CSDNs⁴³ to prevent serotonin release by knocking down Vmat in these cells via expression of Vmat RNAi. Previous work from our lab has shown that endogenous release of 5-HT from the CSDNs modulates activity in the AL,⁴¹ and the expression of the Vmat-RNAi transgene in the CSDNs successfully eliminates these 5-HT-mediated responses in the AL.⁴⁴ To further validate the impact of RNAi knockdown of Vmat on 5-HT signaling in the CSDNs, we immunolabeled the brains of R60F02-Gal4 flies driving either UAS-GFP or UAS-GFP and UAS-Vmat-RNAi (Figure 1C) and compared the relative 5-HT immunofluorescence intensity of the CSDNs (Figure 1D). Flies in which R60F02-Gal4 drove the expression of the Vmat-RNAi had a near-complete loss of 5-HT immunolabeling, whereas 5-HT immunolabeling was intact in brain regions not innervated by the CSDNs as well as in the CSDNs of control flies. 5-HT has been shown to affect odor-evoked responses in the olfactory systems of many species of insects.^{45–49} Chronic CO₂ exposure of flies deprived of CSDN 5-HT output failed to undergo structural plasticity in the V (Figure 1E), suggesting that serotonin release is required for structural plasticity. To further ascertain if serotonin is sufficient to induce structural plasticity following chronic odor exposure, we employed selective 5-HT reuptake inhibitors (SSRIs) like fluoxetine and escitalopram. Both SSRIs are known to slow down 5-HT reuptake at the dosage concentration of 1 μM but only escitalopram is known to increase 5-HT release at this concentration.⁵⁰ While 6-day-old adult flies fail to undergo structural plasticity in the V following chronic CO₂ exposure, flies of the same age treated with an SSRI like fluoxetine or escitalopram undergo structural plasticity (Figure 1F). Together, these results indicate that 5-HT is required and sufficient to induce structural plasticity following chronic odor exposure.

Serotonin modulates the olfactory CPP via multiple receptor targets

Having established that 5-HT plays a role in the olfactory CPP in *Drosophila*, we wished to determine the cellular and molecular targets by which 5-HT was exerting its impact. 5-HT mediates its effect in cells by concentration-dependent activation of its cognate receptors. In *Drosophila*, there are five serotonin receptors (5-HTRs): 5-HT1AR, 5-HT1BR, 5-HT2AR, 5-HT2BR, and 5-HT7R.^{51–54} We systematically interrogated 5-HTR signaling to determine which receptors are involved in mediating structural plasticity during the critical period (Figure 2). For this, we used the same experimental paradigm as before and employed the null mutants of the 5-HTRs generated by a CRISPR knock in strategy to replace all or parts of the gene encoding the 5-HTRs with the GAL4 gene.⁵⁴ Chronic exposure of CO₂ in flies with mutations in the 5-HT1BR and 5-HT7R (Figures 2C and 2F) failed to demonstrate structural plasticity in the V-glomerulus during the critical period. Since the 5-HT2BR homozygous mutants were not viable in our hands, we employed a slightly modified strategy to investigate its effects on CPP. We crossed the heterozygous 5-HT2BR mutants expressing Gal4 under the 5-HT2BR promoter to induce expression of 5-HT2B-RNAi (for genotypes see Table 1). This 5-HT2BR deficient state was sufficient to block structural plasticity in the V-glomerulus during the critical period (Figure 2E). In contrast, we still observed structural plasticity in 5-HT1AR and 5-HT2AR mutants upon chronic CO₂ exposure during the CP (Figures 2B and 2D), indicating that these two receptors do not underlie the effects of 5-HT on early life olfactory plasticity. Together, these results indicate that 5-HT1BR, 5-HT2BR, and 5-HT7R are required during the critical period.

Table 1. Genotypes of flies in the figures

Figure	Genotype	Source
1A and 1B	Gr21a-Mmus\Cd8a.GFP	BDSC #52619
1C and 1D	R60F02-Gal4/10X-UAS-IVS-mCD8::GFP R60F02-Gal4/UAS-Vmat-RNAi,10X-UAS-IVS-mCD8::GFP	R60F02-Gal4 (BDSC #48228) 10X-UAS-IVS-mCD8::GFP (BDSC #32185) UAS-Vmat-RNAi (BDSC #44471) ⁴⁴
1E	Left to right: Canton-S R60F02-Gal4/UAS-Vmat-RNAi w1118;;UAS-Vmat-RNAi P[y[+t7.7]=CaryP]attP2/R60F02-Gal4	Canton-S (BDSC #64349), w1118 (BDSC#5905) P[y[+t7.7]=CaryP]attP2 (BDSC #36303)
1F	Canton-S	-
2A	Canton-S	-
2B	TI{GAL4}5-HT1A{Gal4}/TI{GAL4}5-HT1A [Gal4]	BDSC#86275
2C	TI{GAL4}5-HT1B{Gal4}/TI{GAL4}5-HT1B [Gal4]	BDSC #86276
2D	TI{GAL4}5-HT2A{Gal4}/TI{GAL4}5-HT2A [Gal4]	BDSC #86277
2E	Left to right: UAS-5-HT2B-RNAi; TI{GAL4}5-HT2B{Gal4} w1118; UAS-5-HT2B-RNAi P[y[+t7.7]=Cary P [attp40]; TI{GAL4}5-HT2B - [Gal4]	UAS-5-HT2B-RNAi (BDSC #60488) TI{GAL4}5-HT2B{Gal4} (BDSC #86278) P[y[+t7.7]=CaryP]attp40] (BDSC #36304)
2F	TI{GAL4}5-HT7{Gal4}	BDSC #86279
3A	w1118; 5-HT1A-7xGFP ₁₁ -HA/5-HT1A-(MI1140)- T2A-GAL4,10xUAS-mCD8-GFP	5-HT1A-7xGFP ₁₁ -HA (this study) 5-HT1A-(MI1140)-T2A-GAL4 ⁵⁵
3B	10xUAS-mCD8-GFP/w1118; 5-HT1B- (MI5213) -T2A-Gal4/5-HT1B-7xGFP ₁₁ -HA	10xUAS-mCD8-GFP (BDSC #32189) MiMIC 5213 HT1B T2A Gal4 ⁵⁵ 5-HT1B-7xGFP ₁₁ -HA (this study)
3C	w1118; 10xUAS-mCD8-GFP/+; 5-HT2A- (MI459)-T2A-Gal4/5-HT2A(BFH)-7xGFP ₁₁ -HA	10xUAS-mCD8-GFP (BDSC #32186) 5-HT2A-(MI459)-T2A-Gal4 ⁵⁵ 5-HT2A(BFH)-7xGFP ₁₁ -HA (this study)
3D	w1118; 10xUAS-mCD8-GFP/+; 5-HT2B- (MI6500)-T2A-Gal4/5-HT2B-7xGFP ₁₁ -HA	5-HT2B-(MI6500)-T2A-Gal4 ⁵⁵ 5-HT2B-7xGFP ₁₁ -HA (this study)
3E	w1118; +/-; 5-HT7-(MI215)-T2A-Gal4,10x UAS-mCD8-GFP/5-HT7-7xGFP ₁₁ -HA	5-HT7-(MI215)-T2A-Gal4 ⁵⁵ 5-HT7-7xGFP ₁₁ -HA (this study)
4A	R70A09-GAL4}attP2/10XUAS-IVS-mCD8:: GFP	R70A09-GAL4}attP2 (BDSC #47720)
4B	10xUAS-sfGFP1-10; R70A09-GAL4/ 5-HT7-7xGFP ₁₁ -HA (this study)	10xUAS-sfGFP1-10 (VK00022; BDSC#93189) - Gift from J. Wildonger, University of California, San Diego
4C	NP1227-Gal4 (LN1)/10XQUAS-6XmCherry -HA; R70A09Q/10XUAS-IVS-mCD8::GFP	NP1227-Gal4 (LN1) (DGRC #103945) 10XQUAS-6XmCherry-HA} (BDSC #52269) GMR70A09Q ⁴⁴
4E	NP2426-Gal4 (LN2); UAS-mCherry/ QUAS-mCD8-GFP; R70A09Q	NP2426-Gal4 (LN2) (DGRC #104198) UAS-mCherry (BDSC #59021) QUAS-mCD8-GFP (BDSC #30002)
4G	Left to right: Canton-S R70A09-Gal4/UAS-5HT7-RNAi w1118;;UAS-5HT7-RNAi P[y[+t7.7]=CaryP]attp2/R70A09 -Gal4	UAS-5HT7-RNAi (BDSC #32471) ⁴⁴ P[y[+t7.7]=CaryP]attp2 (BDSC #36303)
4H	Left to right: Canton-S UAS-dunce;;R70A09-Gal4, w1118/UAS-dunce	w, UAS-dunce; +; + was a gift from B.White Lab at NIH. The fly was first described in Cheung et al., 1999 ⁵⁶

(Continued on next page)

Table 1. Continued

Figure	Genotype	Source
4I	Left to right: Canton-S Peb-Gal4; UAS-GABA _B -RNAi; UAS-GABA _B -RNAi Peb-Gal4; UAS-Rdl-RNAi Orco-Gal4/UAS-GABA _B -RNAi; UAS-GABA _B -RNAi, Orco-Gal4/UAS-Rdl-RNAi Peb-Gal4; P{y[+t7.7]=CaryP}attp40 Peb-Gal4;; P{y[+t7.7]=CaryP}attp2 Orco-Gal4/P{y[+t7.7]=CaryP}attp40 Orco-Gal4; P{y[+t7.7]=CaryP}attp2 w1118; UAS-GABA _B -RNAi; UAS-GABA _B -RNAi w1118; UAS-Rdl-RNAi	UAS-GABA _B -RNAi; UAS-GABA _B -RNAi: Gift from Jing Wang ⁵⁷ Peb-Gal4 (BDSC #80570) UAS-Rdl-RNAi (BDSC #52903) ⁵⁸ Orco-Gal4 (BDSC #26818)
5A	UAS-5-HT2B-RNAi; Gr21a-Gal4/5-HT2B-7x-GFP ₁₁ -HA.	Gr21a-Gal4 (BDSC #23890)
5B	UAS-5-HT2B-RNAi; Gr63a-Gal4/5-HT2B-7x-GFP ₁₁ -HA.	Gr63a-Gal4 (BDSC #9943)
5C	Peb-Gal4; UAS-5-HT2B-RNAi; 5-HT2B-7x-GFP ₁₁ -HA.	–
5D	Left to right: Canton-S UAS-5-HT2B-RNAi; Gr21a-Gal4 w1118; UAS-5HT2B-RNAi P{y[+t7.7]=CaryP}attp40; Gr21a-Gal4	–
5E	Left to right: Canton-S UAS-5-HT2B-RNAi/Gr63a-Gal4 w1118; UAS-5HT2B-RNAi P{y[+t7.7]=CaryP}attp40/Gr63a-Gal4	–
5F	Left to right: Canton-S Peb-Gal4; UAS-5HT2B-RNAi UAS-5-HT2B-RNAi/Orco-Gal4 w1118; UAS-5HT2B-RNAi Peb-Gal4; P{y[+t7.7]=CaryP}attp40 P{y[+t7.7]=CaryP}attp40/Orco-Gal4	–
6A and 6B	5-HT2B-7x-GFP ₁₁ -HA	This study
7A	Left to right: Canton-S R60F02-Gal4>UAS-5-HT1B-RNAi Trh-T2A-Gal4>UAS-5-HT1B-RNAi w1118; UAS-5-HT1B-RNAi P{y[+t7.7]=CaryP}attp40; R60F02-Gal4 P{y[+t7.7]=CaryP}attp40; Trh-T2A-Gal4	UAS-5-HT1B-RNAi (BDSC # 51842) ^{58,59} Trh-T2A-Gal4 (BDSC #84694)
7B	Left to right: Canton-S UAS-5-HT1B; R60F02-Gal4 UAS-5-HT1B; + +; R60F02-Gal4	UAS-5-HT1B (BDSC #27632)

All MiMIC lines were a gift from Dr. Herman A. Dierick, Baylor College of Medicine.

Previous studies demonstrated that all five 5-HT receptors are expressed by distinct neuron types in the AL.⁶⁰ These studies relied on GFP expression induced by the Gal4 protein expressed from the endogenous promoter and provided a detailed list of 5-HTRs expressed by distinct cell types in the AL (see Sizemore and Dacks, 2017). Although this approach reveals which cells classes express which 5-HTRs, the method does not easily identify where and when the receptors are trafficked within the neurons. More recently, endogenously tagged receptors for 5-HT1A, 5-HT2A, and 5-HT2B have been designed to conditionally or constitutively tag these receptors and track where they are trafficked but not for 5-HT1B and 5-HT7.⁶¹ We therefore generated flies with an endogenous HA-tag and the GFP₁₁ fragment on 5-HTRs.^{62–64} We employed a CRISPR-Cas9-based strategy^{65,66} to generate these flies (refer to STAR Methods and Table 2 for detailed stra). The split-GFP is an elegant tool that consists of splitting the superfolder GFP (sfGFP) between the beta-strand 10 and 11 to generate two non-fluorescing, self-complementing fragments: GFP₁₋₁₀ and GFP₁₁.^{67,68} Only cells that would simultaneously express both fragments will be able to form the complete sfGFP molecule that would fluoresce (Figure S1A). Additionally, the HA-tagged 5-HTRs would enable us to locate 5-HTR expression in all cells by immunolabeling against HA (Figure S1B). Together, this strategy allows us to simultaneously visualize the localization of 5-HTRs and determine the cell types that express them (Figures S1C–S1F). We found that the expression patterns of these 5-HTR lines labeled using the MiMIC-5HTR-Gal4 drivers to be consistent with previously reported expression patterns of the 5-HTRs^{55,60} using more traditional GAL4/UAS approaches (Figures 3A–3E).

Table 2. Concentration of antibodies used in this study

Name	Type	Species of origin	Dilution	Supplier	Cat. #
Anti-hemagglutinin(HA)	Primary	Mouse	1:500	Thermo Fisher Scientific	26183; RRID: AB_2533049
Anti-5-HT	Primary	Rabbit	1:5000	Immunostar	20080; RRID: AB_572263
Anti-reconstituted GFP	Primary	Mouse	1:1000	Sigma	G6539; RRID: AB_259941
Anti-GFP	Primary	Chicken	1:1000	Abcam	ab13970; RRID: AB_300798
nc82 Antibody	Primary	Mouse	1:50	Developmental Studies Hybridoma Bank (DSHB)	nc82; RRID: AB2314866
N-cadherin (n-cad)	Primary	Rat	1:50	Developmental Studies Hybridoma Bank (DSHB)	DN-EX #8; RRID: AB_528121
Anti-chicken Alexa Fluor 488	Secondary	Goat	1:400	Thermo Fisher Scientific	A-11039; RRID: AB_2534096
Anti-mouse Alexa Fluor 488	Secondary	Goat	1:400	Thermo Fisher Scientific	A-11004; RRID: AB_2534072
Anti-rabbit Alexa Fluor 546	Secondary	Donkey	1:1000	Thermo Fisher Scientific	A-10040; RRID: AB_2534016
Anti-mouse Alexa Fluor 633	Secondary	Goat	1:400	Thermo Fisher Scientific	A-21050; RRID: AB_2535718

Next, we investigated the differential expression patterns of the 5-HTRs in the olfactory processing centers of the brain. The 5-HT1Rs are expressed in varying degrees within the AL and MBs (Figure 3A). The 5-HT2ARs are mostly expressed in the cells surrounding and innervating the AL, most likely the LNs and PNs (Figures 3C' and 3Cc'). Remarkably 5-HT2BRs is not uniformly expressed throughout the AL (Figures 3D', 3Dd', and S2A–S2I). This indicates varying levels of 5-HT2BR-mediated serotonergic modulation in the OSNs. Consistent with prior reports,⁶⁰ we found most of the 5-HT2BR expression in the AL to be in the OSNs. When we removed the antennae or the maxillary palps that houses the cell body and dendrites of OSNs, 5-HT2BR expression in the related AL region the OSNs project to is eliminated (Figure S2J). Similarly, we were able to selectively knockdown 5-HT2BRs expression using Gal4 drivers for OSN subtypes using an RNAi against 5-HT2BR (Figures S2K and S2L). The AL neuropil is innervated by various cells including OSNs, PNs, LNs, and CSDNs. We found most of the 5-HT7R expression in the cells surrounding the AL, most likely in the LNs and PNs (Figures 3E' and 3E''). We also found unusually high GFP labeling in two glomeruli in the AL (Figure 3E''') but no corresponding HA labeling (Figure 3Ee''') for 5HT7R expression using the MIMIC-5HT7R-Gal4 promoter line. Taken together, these results show that 5-HT targets multiple components of olfactory processing through distinct receptors. Therefore, serotonin could target multiple serotonergic receptors on distinct cell types to mediate their effects during the olfactory critical period.

Serotonin modulates distinct components of sensory processing during the critical period

Next, we wanted to isolate the neuronal basis of 5-HTR signaling that modulates CPP. Earlier studies have identified a crucial role of inhibitory, GABAergic LNs, namely LN1 and LN2, during the olfactory critical period.^{20,21,27} Previous work in our lab has identified a distinct population of 5-HT7R-expressing GABAergic LNs (R70A09-Gal4) that are responsive to low 5-HT concentrations and modify odor coding in the AL.⁴⁴ As a population, these LNs innervate all glomeruli including the V-glomerulus (Figure 4A). We also found that R70A09-GAL4 LNs express 5-HT7Rs (Figure 4B) and show almost a complete overlap with LN1 neurons (Figures 4C and 4D) and a partial overlap with the LN2 neurons (Figures 4E and 4F). The LN1 neurons have been previously implicated to induce an increase in the number of PN arbors leading to structural plasticity during the critical period.^{20,21} We therefore sought to determine if these LNs are the target for 5-HT modulation via the 5-HT7Rs and found that knocking down 5-HT7Rs in the R70A09 LNs was sufficient to prevent CPP in the V-glomerulus (Figure 4G). In *Drosophila*, 5-HT7Rs are known to activate an adenylate cyclase that results in an increase in cytosolic cAMP.^{51,69} When we overexpress the cAMP-specific phosphodiesterase *dunce* to deplete cAMP selectively in the R70A09 LNs, keeping the 5-HT7Rs and adenylate cyclase intact, CPP in the V-glomerulus is abolished (Figure 3H). These results indicate that both 5-HT7R signaling and cAMP in R70A09-GAL4 LNs play an important role during the CP that ultimately permits the induction of structural plasticity in the cognate glomerulus.

The R70A09 LNs that express 5-HT7 receptors are GABAergic in nature and release GABA upon activation.⁴⁴ The pan-glomerular innervation of these LNs implies that they release GABA all over the AL. Apart from these LNs, other GABAergic LNs also exist in the AL that can be sensitive to serotonergic modulation. Previous work has shown that GABA released from the GH298 LNs that are distinct from the R70A09 LNs mediate glomerulus selective presynaptic divisive gain control in Or83b-expressing OSNs in adult *Drosophila* but do not affect CO₂ responses in the Gr21a-expressing OSNs.⁵⁷ Consistent with these studies, knocking down GABA_B and GABA_A receptors, respectively, in the CO₂-sensing OSNs and PNs was not sufficient to block structural plasticity during the CP.^{20,23} However, 5-HT7R-mediated activation in the R70A09 LNs and thereby GABA release is important for inducing CPP. Therefore, it is likely that R70A09 LN-activation-linked GABA release during the critical period could lead to network level changes in the AL that ultimately facilitate structural plasticity in the cognate glomerulus. We asked if the two GABA receptors expressed in the fly, the GABA_A and GABA_B receptors, are required for global inhibition in the OSNs during the critical period. When we knock down GABA_B receptors in all OSNs, we saw no structural plasticity in the V-glomerulus (Figure 4I). In contrast, knocking down GABA_A receptors in all OSNs did not hinder CPP in the V (Figure 4I). Finally, we targeted Or83b OSNs in the AL using the Orco-Gal4 promoter line. This enabled targeting multiple OSNs responsive to different odors^{44,57} but not the CO₂ sensing

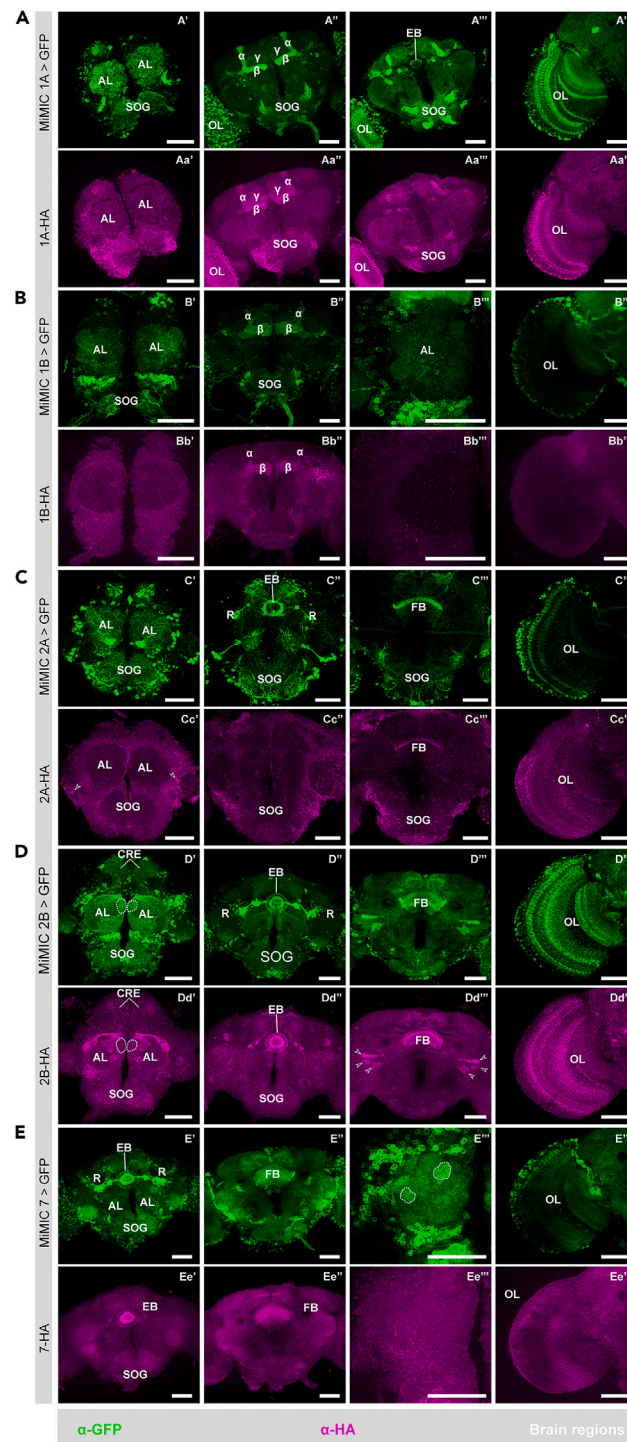


Figure 3. Distribution of 5-HTRs in adult *D. melanogaster* brains

(A) Brain sections indicate 5-HT1A expression in the AL, subesophageal ganglion (SOG), MB, ellipsoid body (EB), and optic lobe (OL). As shown in (A'') and (Aa''), both α -HA and α -GFP indicate expression in all three lobes of MB, including α , β , and γ lobes. Note, as shown in (Aa'''), 5-HT1A expression in EB is largely devoid revealed by α -HA, contrary to the α -GFP staining pattern shown in (A''').

(B) Brain sections indicate 5-HT1B expression in SOG, AL, MB, and OL. In contrast to the MiMIC approach, which labels cell bodies broadly in the brain, immunostaining against the HA tag show significant distribution of the receptor only in the α and β lobes of MB.

Figure 3. Continued

(C) Brain sections indicate 5-HT2A expression in many areas such as AL, SOG, EB, the fan-shaped body (FB), and optical lobe (OL). Among all these areas, the staining by α -HA shows weak signals in FB (Cc''') and probably in OL (Cc''', indicated by the arrow heads). The contrast of the images from the α -HA channel was elevated to see weak signals, resulting in irregular signal presentation that might be artifacts, as indicated by the arrow heads in (Cc'-Cc''').

(D) Brain sections indicate 5-HT2B expression in AL, crepines (CRE), SOG, EB, FB, and OL. In ALs, the MiMIC approach indicates a relatively high expression in a medial glomerulus, as emphasized by the white dashed circle, which is not consistent in the α -HA channel (Dd'). It is noticeable that localization of this receptor in the R neurons (R) and their arborizations toward EB (D'', arrow heads) is missing in the staining pattern revealed by α -HA (Dd''). Arrow heads in (D'') and (Dd'') indicate some unknown structures stained in both channels.

(E) Brain sections indicate 5-HT7 expression in SOG, EB, FB, and (E'''/Ee''') OL. In the antennal lobe labeled with the MiMIC approach, extraordinary signals were observed in an anterior dorsal glomerulus as indicated by dashed circle on the right side and a posterior lateral glomerulus as indicated by dashed circle on the left side (E'''). In contrast, no prominent signals showed in these two glomeruli as indicated by the α -HA approach (Ee'''). Signals were observed in the optical lobe (OL) revealed by both approaches (E'''/Ee'''). For both (E'''/Ee''') and (E'''/Ee'''), the brain was oriented with the lateral toward left and the dorsal upward. The scale bar indicates 50 μ m in all cases. Detailed genotypes of flies for each experimental condition can be found in Table 1 and the antibody concentrations used in Table 2.

ones. Surprisingly, flies expressing GABA_A RNAi in Or83b OSNs failed to undergo structural plasticity in the V upon CO₂ exposure (Figure 4H). However, knocking down GABA_B in the Or83b OSNs was not sufficient to prevent structural plasticity in the V in response to CO₂ (Figure 4I). This shows that GABAergic inhibition during the critical period via GABA_A is required in a broader sub-population of OSNs in the AL but not selectively in the cognate glomerulus because Or83b OSNs do not innervate the V and few other glomeruli. On the other hand, GABAergic inhibition via GABA_B is required in all OSNs in the AL including the V glomerulus, as *Peb-Gal4* is expressed in all OSNs. Therefore, GABA targets distinct OSNs through GABA_A and GABA_B receptors to facilitate CPP in the V glomerulus.

Next, we asked which cells projecting to the AL could be the source of 5-HT2BR-mediated serotonergic modulation of the olfactory CPP. We hypothesized that 5-HT targets 5-HT2BRs on OSNs during the critical period. Previous research has shown that the 5-HT2BRs are expressed by all OSNs and a few LNs and PNs in the AL.⁶⁰ We showed earlier in Figure S2J that the majority of the 5-HT2BR expression in the antennal lobe is due to their expression by the OSNs. Therefore, we selectively knocked down expression of the 5-HT2BRs in the V-glomerulus OSNs (Figure 5). In the CO₂-detecting OSNs, two chemoreceptors, Gr21a and Gr63a, are co-expressed to form a functional CO₂ responsive odor receptor.⁷⁰ However, in our 5-HT2BR knockdown experiments, we observed residual 5-HT2BR expression in the V-glomerulus using the Gr21a-GAL4 driver line (Figure 5A). Therefore, 5-HT2BR knockdown driven by the Gr21a-Gal4 line was not sufficient to prevent CPP in the V-glomerulus (Figure 5D). In contrast, driving the 5-HT2BR RNAi using Gr63a-Gal4 significantly reduced 5-HT2BR expression in the V-glomerulus without impacting expression in the rest of the AL (Figure 5B). This selective knockdown of the 5-HT2BRs by the Gr63a-Gal4 line was sufficient to prevent the induction of structural plasticity in the V-glomerulus (Figure 5E), suggesting that 5-HT2BR expression is required by OSNs within the glomerulus expanding during the CP. To determine if 5-HT2BR expression by OSNs in other glomeruli is required for CPP in the V-glomerulus, we next extended the 5-HT2BR knockdown using drivers expressed broadly in all OSNs (*Peb-Gal4*) or in many OSNs, except those projecting to the V and a few other glomeruli (*Orco-Gal4*). We found that flies that expressed 5-HT2B RNAi in all OSNs (Figure 5C) failed to undergo structural plasticity in the V-glomerulus in response to chronic CO₂ exposure (Figure 5F). In contrast, 5-HT2B knockdown in multiple OSNs using the *Orco-Gal4* driver line did not show any deficits in structural plasticity in response to CO₂ (Figure 5F). Together, these results show that the 5-HT2BR expression is required in cognate ORNs of the V glomerulus for proper expression of CPP.

We also observed glomerulus specific differences in the expression levels of the 5-HT2BRs. (Figures S2A–S2I). Therefore, to determine if expression of the 5-HT2BRs within the AL varies post-eclosion, we employed the 5-HT2BR-HA-tagged recombinant flies. We found that the expression of the 5-HT2BRs increases significantly post-eclosion and reaches its peak at day 2 or 48 h post-eclosion (Figures 6A and 6B), which coincides with the closing of the critical period.^{21,27} After day 2, the 5-HT2BR expression does not vary significantly, as we saw no difference in the corrected total fluorescence between day 2, day 4, and day 5 post-eclosion. Taken together, these results show that 5-HT targets both excitatory and inhibitory neurons within the antennal lobe via distinct receptors.

Autoregulation of serotonergic neurons during the critical period

Finally, we sought to determine the neurons for whom expression of the 5-HT1BR is required for the olfactory CPP. Within serotonergic neurons, the 5-HT1BRs often act as auto receptors by either inhibiting the release of 5-HT^{71–74} or modulating serotonin reuptake by upregulating SERT activity and clearance rate.⁷⁵ Therefore, we knocked down 5-HT1B receptors in the CSDns, release of 5-HT from which is required during critical period (Figure 7A). We found that 5-HT1B signaling in CSDns is required for glomerular-specific volume increase during the critical period. Similarly, knocking down 5-HT1BRs in all serotonergic neurons in the brain using a Gal4 promoter line *Trh-Gal4* was able to block CPP in the V-glomerulus (Figure 7A). The CSDns release 5-HT upon activation. Since the 5-HT1BRs are inhibitory in nature, activation of 5-HT1BRs on CSDns will inhibit 5-HT release from them. We also know that release of 5-HT from the CSDns is important during the critical period. Therefore, if we overexpress 5-HT1BRs in the CSDns, there will be a stronger inhibition in the CSDns most likely preventing CPP. Consistent with our hypothesis, we saw that 5-HT1BR overexpression on CSDns prevents CPP in the V-glomerulus following CO₂ exposure (Figure 7B). Together, these results indicate that 5-HT levels need to be tightly controlled to induce CPP.

DISCUSSION

There are many cellular and molecular components that contribute to CPP. Serotonin is elegantly positioned to affect CPP because a diverse set of 5-HT receptors are broadly expressed throughout the network. The genetically accessible olfactory circuit of *Drosophila* allowed us to

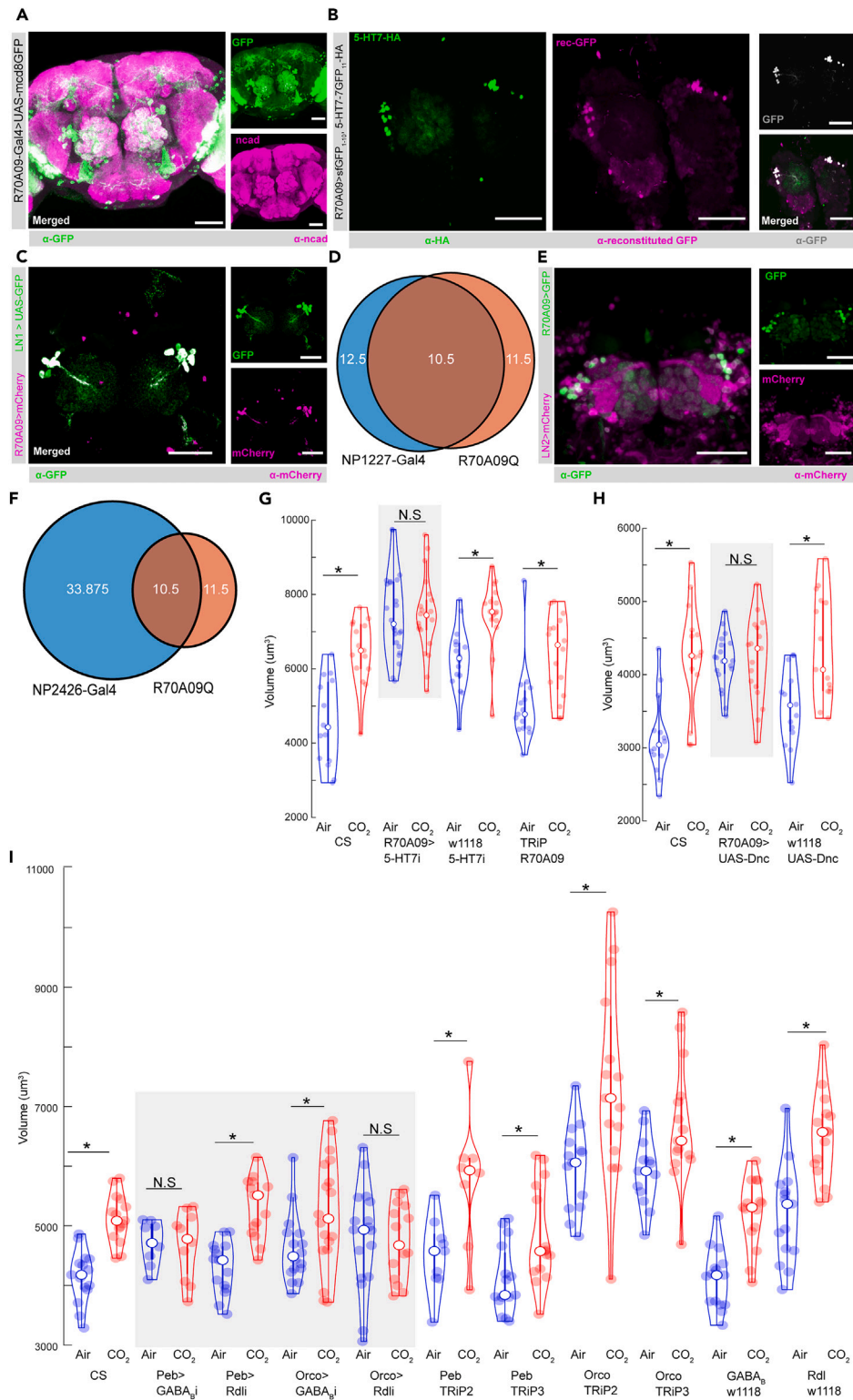


Figure 4. 5-HT7 targets GABAergic inhibition in the primary olfactory circuit

(A) Confocal maximum intensity projection of the R70A09 LNs expressing GFP in green, co-labeled for n-cadherin in magenta. The V-glomerulus is circled in the merged and GFP channels.

Figure 4. Continued

- (B) Confocal maximum intensity projection of the AL showing R70A09 LNs co-labeled for 5-HT7-HA in green, reconstituted GFP in magenta, GFP in gray, and the merged channel.
- (C) Confocal maximum intensity projection of the AL showing the overlap between R70A09 LNs in magenta and LN1 neurons in green.
- (D) The R70A09 line labels 11–12 LNs, LN1 labels 12–15 LNs per hemisphere. There is a total overlap of 10–11 cells between R70A09 and LN1 population per hemisphere.
- (E) Confocal maximum intensity projection of the AL showing the overlap between R70A09 LNs in green and LN2 in magenta.
- (F) The R70A09 line labels 11–12 LNs, LN2 labels 33–44 LNs per hemisphere. There is a total overlap of 10–11 cells between R70A09 and either LN1 or LN2 population per hemisphere.
- (G) Quantification of V glomerulus volumes comparing air- and 5% CO₂-exposed flies during the critical period. Four genotypes are shown here from left to right: CS (Canton-S wildtype), R70A09>5-HT7i (R70A09 targeted 5-HT7 knockdown), w1118 5-HT7i (background control for Gal4), and TRiP R70A09 (background control for RNAi).
- (H) Comparison of V-glomerulus volumes in air- and 5% CO₂-exposed brains of flies with overexpression of *dunce* in the R70A09 LNs. Three genotypes are shown here from left to right: CS (Canton-S wildtype), R70A09>UAS-Dnc (*dunce* overexpression in R70A09 LNs), and w1118 UAS-Dnc (background for Dnc and R70A09).
- (I) Comparison of V-glomerulus volumes in air- and 5% CO₂-exposed brains of flies with GABA receptor knockdown in OSNs. Eleven genotypes are shown here from left to right: CS (Canton-S wildtype), *Peb>GABA_Bi* (GABA_B knockdown in all OSNs), *Peb>Rdli* (GABA_A knockdown in all OSNs), *Orco>GABA_Bi* (GABA_B knockdown in Or83b OSNs), *Orco>Rdli* (GABA_A knockdown in Or83b OSNs), *Peb TRiP2* (background control for Rdl RNAi crossed with *Peb-Gal4*), *Peb TRiP3* (background control for GABA_B RNAi crossed with *Peb-Gal4*), *Orco TRiP2* (background control for Rdl RNAi crossed with *Orco-Gal4*), *Peb TRiP3* (background control for GABA_B RNAi crossed with *Orco-Gal4*), w1118 GABA_Bi (background for Gal4 crossed with GABA_B-RNAi), and w1118 Rdli (background for Gal4 crossed with Rdl-RNAi). * indicates $p < 0.05$; N.S indicates $p > 0.05$. $n \geq 15$. All violin plots include individual data points (colored circles) and mean (white circle). The boxplot of the data is also represented at the center of the violin. The scale bar indicates 50 μm , and gray boxes indicate experimental fly lines in all cases. Detailed genotypes of flies for each experimental condition can be found in Table 1 and the antibody concentrations used in Table 2.

isolate the effects of serotonergic modulation in the critical period exclusively within the olfactory circuit via regulating serotonin release from the CSDNs and selectively knocking down 5-HTRs in specific cell types within the olfactory circuit. We first showed that 5-HT is required to induce structural plasticity following chronic odor exposure. Second, we showed that three out of the five 5-HTRs are required for CPP in different neurons. Although 5-HT7Rs are required on a specific subset of LNs that mediate cAMP-dependent structural plasticity during the critical period, the 5-HT2BRs are required in the cognate OSNs, and their expression within the OSNs gradually increases post-eclosion and reaches its peak at the end of the critical period. Furthermore, 5-HT1BRs are required in the serotonergic neurons CSDNs. Finally, using SSRIs, we were able to induce structural plasticity in 6-day-old adults when the critical period is normally closed. These results indicate that 5-HT is necessary to induce CPP, and it differentially modulates both excitatory and inhibitory elements in the olfactory circuit during the critical period.

5-HT modulates inhibitory LN circuits that underlie critical period plasticity

Critical periods are known to be tightly regulated by the maturation of inhibitory circuits. In fact, the emergence and maturation of GABAergic inhibitory local interneurons (LNs) in mammals^{30,76} are known to improve the signal-to-noise ratio by improving their excitation/inhibition balance³⁰ in visual,⁷⁷ auditory,²⁹ and somatosensory⁷⁸ cortices during the critical period. Previous investigations of the olfactory critical period in *Drosophila* have identified a key role of two distinct inhibitory, GABAergic LN populations (LN1 and LN2) in modulating PN output and structural plasticity upon chronic odor exposure during the critical period.^{20,27} The LN1 sub-population labeled by the NP1227 Gal4 line showed small, statistically insignificant increments in its dose-response curve during chronic CO₂ exposure. In contrast, the LN2 LNs labeled by the NP2426-Gal4 line showed significant increases in its cytosolic Ca²⁺ upon chronic CO₂ exposure during the critical period.²⁷ We identified that 5-HT7R-mediated serotonergic modulation within this circuit activates cAMP-dependent mechanisms of gene expression in LN1 neurons that then induces the volume changes.

The CSDNs maintain reciprocal connections with the inhibitory, GABAergic, and glutamatergic LNs within the AL.³⁸ These LNs are critical for network level inhibition in the AL, as they tone down PN output before it reaches the MB and LH.^{57,79–84} Following odor exposure, CSDN inhibits some LN types via 5-HT. In turn, the CSDNs are inhibited by both GABAergic and glutamatergic inhibition.⁴¹ Thus, the CSDNs could modulate network level inhibition in the AL via serotonergic modulation and can themselves undergo inhibition based on the network-wide inhibitory dynamics established by the LNs. While blocking 5-HT release from the CSDNs prevented the availability of synaptic 5-HT and thereby CPP, the AL neurons also had access to basal 5-HT levels released by the remaining 108 serotonergic neurons in *Drosophila*. A prime candidate of basal 5-HT modulation is the 5-HT7R-expressing R70A09 GABAergic LNs we identified to be required during the critical period.⁴⁴ These R70A09 LNs mediate subtractive gain control in the PNs and thereby downregulate global PN responses.⁴⁴ Our results indicate that although the basal 5-HT levels are trivial during the critical period, 5-HT7R-mediated modulation of R70A09 is required during the critical period. This implies that these cells are most likely playing a crucial role during the critical period in maintaining the inhibitory tone in the AL that is conducive to structural plasticity during the critical period.

In *Drosophila*, the Ca²⁺/calmodulin-sensitive adenylate cyclase rutabaga (*rut*) acts as a coincidence detector for cytosolic Ca²⁺ increase and GPCR activation^{20,85} and converts ATP to cAMP. Rescuing (*rut*) in LN1 or GABA-expressing glutamic acid decarboxylase (GAD-1)-positive

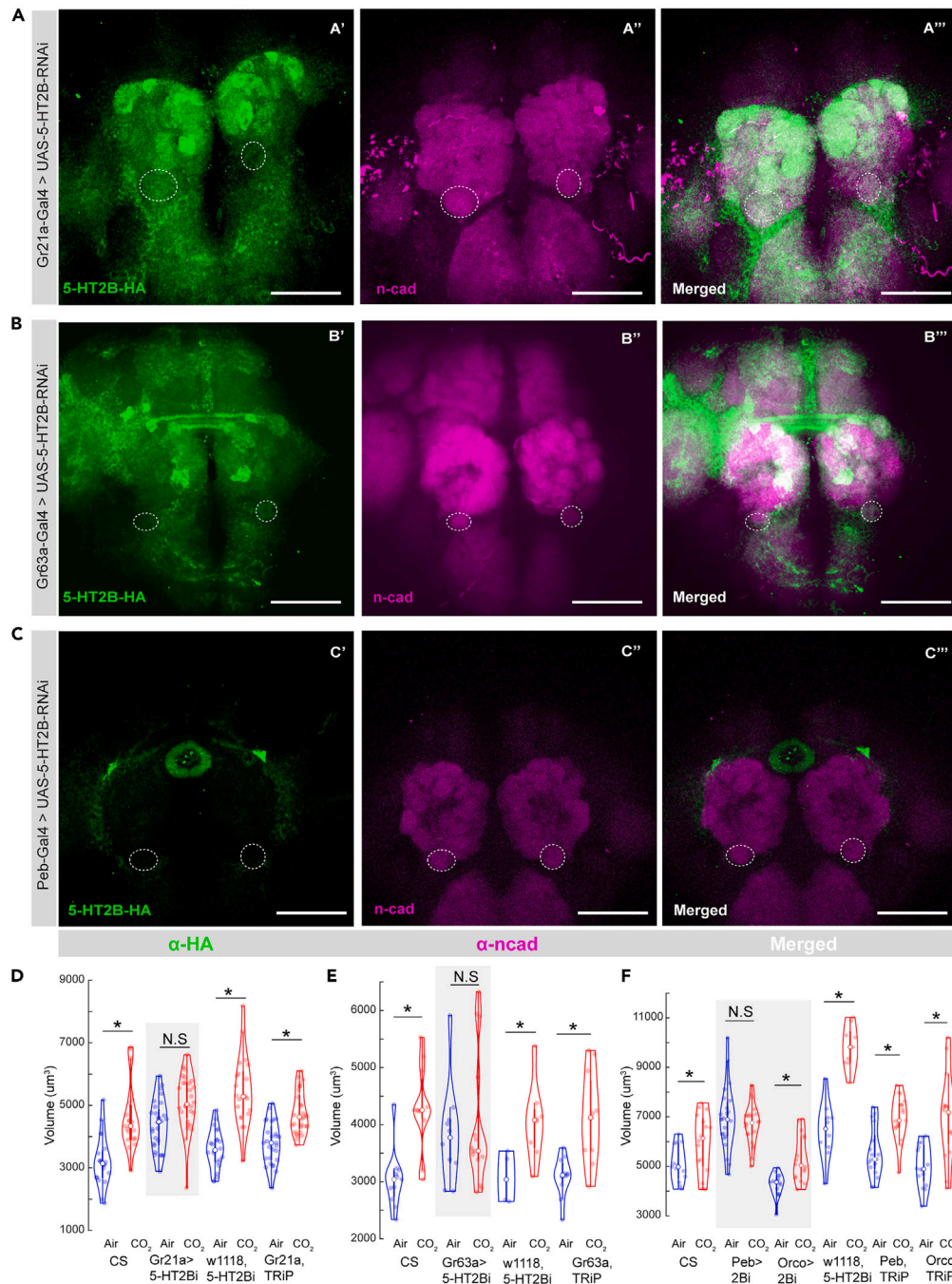


Figure 5. 5-HT2BRs are required in OSNs during the critical period

(A) Insufficient 5-HT2B knockdown in the CO₂-sensing OSNs by Gr21a-Gal4. The V glomerulus is circled on all three channels.

(B) 5-HT2B knockdown in the CO₂-sensing OSNs by Gr63a-Gal4. The V glomerulus is circled on all three channels.

(C) 5-HT2B knockdown in all OSNs but no other brain regions by Peb-Gal4. The V glomerulus is circled on the n-cad (magenta) and merged channels.

(D) Quantification of V glomerulus volumes comparing air- and 5% CO₂-exposed flies during the critical period. Four genotypes are shown here from left to right: CS (Canton-S wildtype), Gr21a>5-HT2Bi (5-HT2B knockdown in CO₂ OSNs), w1118 5-HT2Bi (background control for Gal4), and Gr21a, TRIP (background control for RNAi).

(E) Quantification of V glomerulus volumes comparing air- and 5% CO₂-exposed flies during the critical period. Four genotypes are shown here from left to right: CS (Canton-S wildtype), Gr63a>5-HT2Bi (5-HT2B knockdown in CO₂ OSNs), w1118, 5-HT2Bi (background control for Gal4), and Gr63a, TRIP (background control for RNAi).

Figure 5. Continued

(F) Quantification of V glomerulus volumes comparing air- and 5% CO₂-exposed flies during the critical period. Six genotypes are shown here from left to right: CS (Canton-S wildtype), *Peb>5-HT2Bi* (5-HT2B knockdown in all OSNs), *Orco> 2Bi* (5-HT2B knockdown in Or83b OSNs), *w1118,5-HT2Bi* (background control for Gal4), *Peb, TRiP* (background control for 5-HT2B-RNAi), and *Orco, TRiP* (background control for 5-HT2B-RNAi). * indicates $p < 0.05$; N.S indicates $p > 0.05$. $n \geq 15$. The scale bar indicates 50 μm , and gray boxes indicate experimental fly lines in all cases. All violin plots include individual data points (colored circles) and mean (white circle). The boxplot of the data is also represented at the center of the violin. Detailed genotypes of flies for each experimental condition can be found in Table 1 and the antibody concentrations used in Table 2.

neurons in *rut²⁰⁸⁰* mutants was sufficient to reinstate CPP in those flies.^{20,21} We found almost a complete overlap between 5-HT7-expressing R70A09 LNs and the LN1 neurons. Therefore, we can presume a serotonergic modulation in LN1 and consequently in the R70A09 LNs to be acting via 5-HT7-mediated cAMP increase that results in CREB-dependent gene transcription. Our results show that depleting cAMP while keeping the 5-HT7Rs intact in the R70A09 LNs was sufficient to block CPP. The known organisms across phyla that express 5-HT7, all employ an adenylate-cyclase-dependent mechanism to increase cytosolic cAMP.^{51,69,86–97} Within the LN1 neurons, the adenylate cyclase *rutabaga* is required for CPP.^{20,21} It is likely that 5-HT7Rs expressed in these LNs modulate cAMP-dependent gene transcription to facilitate structural plasticity during the critical period. This is also consistent with the known mechanism of 5-HT7R activity, which increases intracellular cAMP levels in *Drosophila*.⁶⁹ Future work is required to identify if 5-HT7Rs in *Drosophila* acts through the adenylate cyclase *rutabaga* to induce CREB-dependent structural plasticity in the R70A09/LN1 neurons.

5-HT directly modulates excitatory OSNs during the critical period

5-HT can modulate circuits directly by acting through 5-HTRs expressed by neurons in the circuit and/or indirectly by modulating 5-HTRs on neurons that feedback onto the neuronal circuit. Within the AL, we see that in addition to impacting local interactions, 5-HT also directly impacts 5-HT2BRs on OSNs during the critical period, suggesting that there is direct modulation of primary sensory afferents by 5-HT. The differential expression levels exhibited by 5-HT2BRs following eclosion and until the end of the critical period (2 days post eclosion) in the AL is reminiscent of the patchy temporal expression of 5-HT2CRs in the kitten striatal cortex during the visual critical period.³³ Since the ORNs are the primary source of 5-HT2BR expression in the AL, it is likely that the 5-HT2BR-mediated serotonergic modulation adapts specifically to the odor environment presented to the fly during the critical period. This explains why knocking down 5-HT2BRs in the CO₂-responsive OSNs prevents CPP in its cognate V-glomerulus. These results indicate that lower levels of 5-HT2BR expression are permissive to CPP, whereas higher levels of 5-HT2BR signaling beyond the critical levels achieved at day 2 prevent CPP. Additionally, we found differential, patchy expression patterns of the 5-HT2BRs in distinct glomeruli of the antennal lobe during the critical period and in adults, which could also indicate odor-dependent differential serotonergic modulation within distinct glomerulus in the AL. Future work directly correlating 5-HT2BR expression in individual glomerulus with the induction of CPP can shed light on the exact levels of 5-HT2BR modulation required during the critical period. Since the CO₂-sensing OSNs do not undergo structural plasticity during the critical period,²⁷ downstream pathways by which 5-HT2BRs modulate OSNs during the critical period might shed light on how they indirectly affect structural plasticity in the LNs and PNs. The most likely mechanism could be via NMDA-receptor-dependent coincident detection that plays an important role in mediating glomerulus-specific volume increase during the critical period.^{20,21,27} Thus, 5-HT can differentially modulate distinct glomeruli based on their 5-HT2BR expression levels upon a specific odor encounter during the critical period.

Maintenance of optimum serotonin levels during the critical period

The balance of excitation and inhibition (E/I) within a network is fundamentally important for facilitating critical period plasticity.^{98,99} Intracellular electrophysiological recordings in mice indicate 5-HT acts by differentially modulating relevant excitatory and inhibitory synapses during the critical period.¹⁰⁰ This indicates that 5-HT levels can play an important role in controlling permissive levels of excitation and inhibition during the critical period. Therefore, 5-HT levels and thereby 5-HT release permissive to CPP need to be tightly controlled. Similar effects of dopamine are observed during a critical period of sleep in *Drosophila* that helps in the proper development of a glomerulus intricately involved with courtship.¹⁰¹ Serotonin neurons are known to be modulated by 5-HT itself via expression of 5-HTRs.⁶⁹ We show direct evidence of how serotonergic neurons modulate their own release to achieve optimum 5-HT levels through autoregulation. In the larval *Drosophila* nociceptive circuit, the inhibitory 5-HT1BRs expressed in a pair of serotonergic neurons directly inhibit sensory afferents and facilitate a form of experience-dependent plasticity.¹⁰² Similarly, the 5-HT1BRs are expressed by the CSDns,⁶⁹ and knocking down (Figure 7A) or overexpressing the 5-HT1BR in the CSDns (Figure 7B) prevents CPP. Additionally, knocking down 5-HT1B neurons globally in all serotonergic neurons has the same effect (Figure 7A). The inhibitory nature of the 5-HT1BRs implies that the reduction of 5-HT release is required to facilitate CPP. On the other hand, overexpressing 5-HT1BRs on CSDNs ensures less 5-HT release, and because 5-HT release from the CSDNs is required for CPP (Figure 1D), we can conclude that 5-HT levels are carefully regulated during the critical period to maintain permissive levels of E/I balance. This concentration-dependent, bi-directional control allows for the maintenance of an optimal 5-HT level above or below which CPP is hindered.

An alternate mode of action of the 5-HT1BRs on serotonergic cells could be the localization of the serotonin transporters (dSERTs) that promote serotonin reuptake, thereby reducing extracellular 5-HT levels.^{71,72,74} Further studies are required to confirm if this mechanism holds true for serotonergic modulation of serotonin neurons during the critical period.

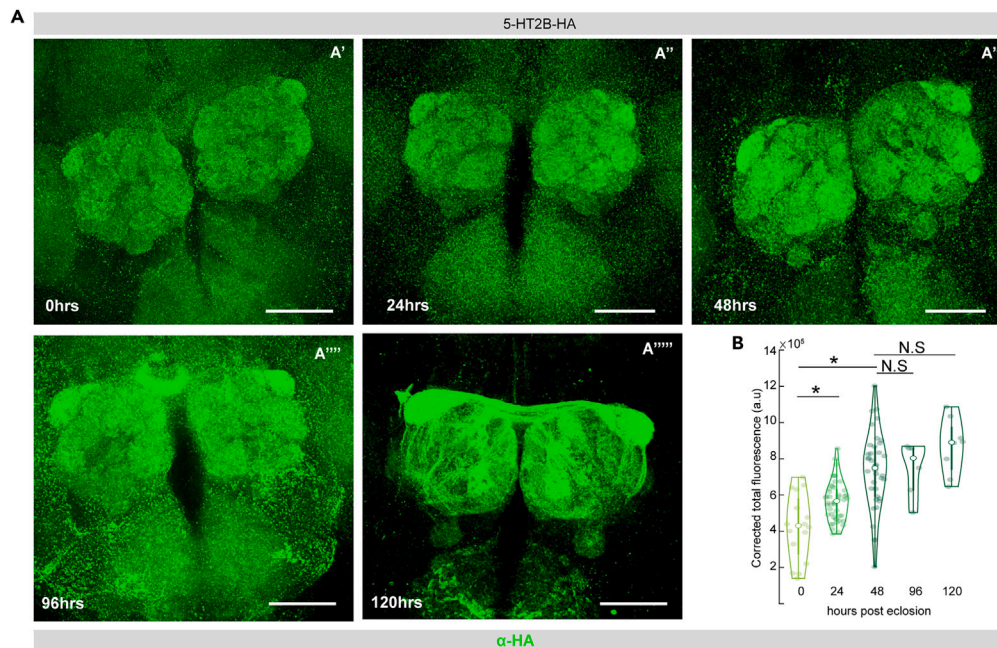


Figure 6. 5-HT2BR expression in the AL varies during the critical period

(A) 5-HT2B expression levels in the AL as indicated by HA staining in green at different life stages of the fly post eclosion: 0 h or freshly eclosed (A') 24 h (A''), 48 h (A'''), 96 h (A''''), and 120 h (A''''').

(B) Total corrected cell fluorescence indicating 5-HT2B expression levels in the AL of the fly at different ages from left to right: 0 h or freshly eclosed, 1 day or 24 h post-eclosion (p.e.), 2 days or 48 h p.e., 4 days or 96 h p.e., and 5 days or 120 h p.e.** indicates $p < 0.05$; N.S indicates $p > 0.05$. The scale bar indicates 50 μm in all cases. $n \geq 15$. All violin plots include individual data points (colored circles) and mean (white circle). The boxplot of the data is also represented at the center of the violin. Detailed genotypes of flies for each experimental condition can be found in Table 1 and the antibody concentrations used in Table 2.

Neuronal mechanism of serotonergic modulation in CPP

During the olfactory critical period, chronic activation of the OSNs by an odor leads to activation-dependent structural plasticity in the cognate glomerulus. This increase in volume can be attributed to the increase in PN and LN arborizations in an odor-specific manner.^{19–21,27} In a specific subpopulation of GABAergic LNs, the LN1 neurons, the adenylate cyclase *rutabaga* increases cAMP levels to promote CREB-dependent gene transcription. This facilitates the structural plasticity observed in both the LNs and PNs.²⁰ Functionally, it leads to an increase in inhibitory output and a decrease in excitatory PN output onto the higher order olfactory centers. This mechanism suggests a way by which the primary olfactory center modulates sensory output before it can reach the second-order olfactory centers (Figure 7C). Our observations show that serotonergic modulation integrates at multiple levels of this model to modify the output from the AL. Firstly, 5-HT release from the CSDNs within this circuit is required for the structural plasticity. Additionally, 5-HT levels in the extracellular space are maintained by 5-HT1BR-mediated inhibition of serotonergic neurons. Similarly, serotonergic modulation on the OSNs is tightly controlled where lower levels of 5-HT2BR expression permit structural plasticity while higher levels of 5-HT2BR expression achieved 2 days post-eclosion coincide with the end of the critical period. The 5-HT7Rs on the R70A09 LNs and therefore the LN1 neurons likely activate cAMP-dependent gene transcription that ultimately leads to the increase in LN and PN arborizations, resulting in glomerular volume increase (Figure 7D). It is still unclear how 5-HT release from the CSDNs gives rise to glomerulus-specific plasticity. The most logical explanation supported by prior literature relies on coincidence detection. Simultaneous activation of OSNs and LNs in the same glomerulus imparts glomerular specificity, which is then modulated by 5-HT2BRs on OSNs. Future experiments are required to examine this model at a greater detail at the cellular and molecular level using pharmacology and electrophysiology.

In conclusion, our work provides insight into how 5-HT modulates structural plasticity at multiple sites of primary olfactory processing during the olfactory critical period. Specifically, we show that 5-HT directly affects the stimulus specific circuit via 5-HT2BRs on the OSNs and 5-HT7Rs on LNs, which indirectly modulates GABAergic inhibition throughout the AL. We also show that 5-HT release from the CSDNs is carefully controlled during the critical period, disruption of which hinders CPP. This supports the view that neuromodulators affect different components of sensory processing to facilitate structural plasticity during the critical period.

Limitations of this study

We should note that we tested the effect of 5-HT on a limited number of cell types within the antennal lobe that we hypothesized to be involved in critical period plasticity within the context of the CO₂-sensing circuit. Future experiments are required to test the effects of serotonergic modulation on other cell types like PNs and other LN subtypes during the critical period on olfactory processing. Additionally, here

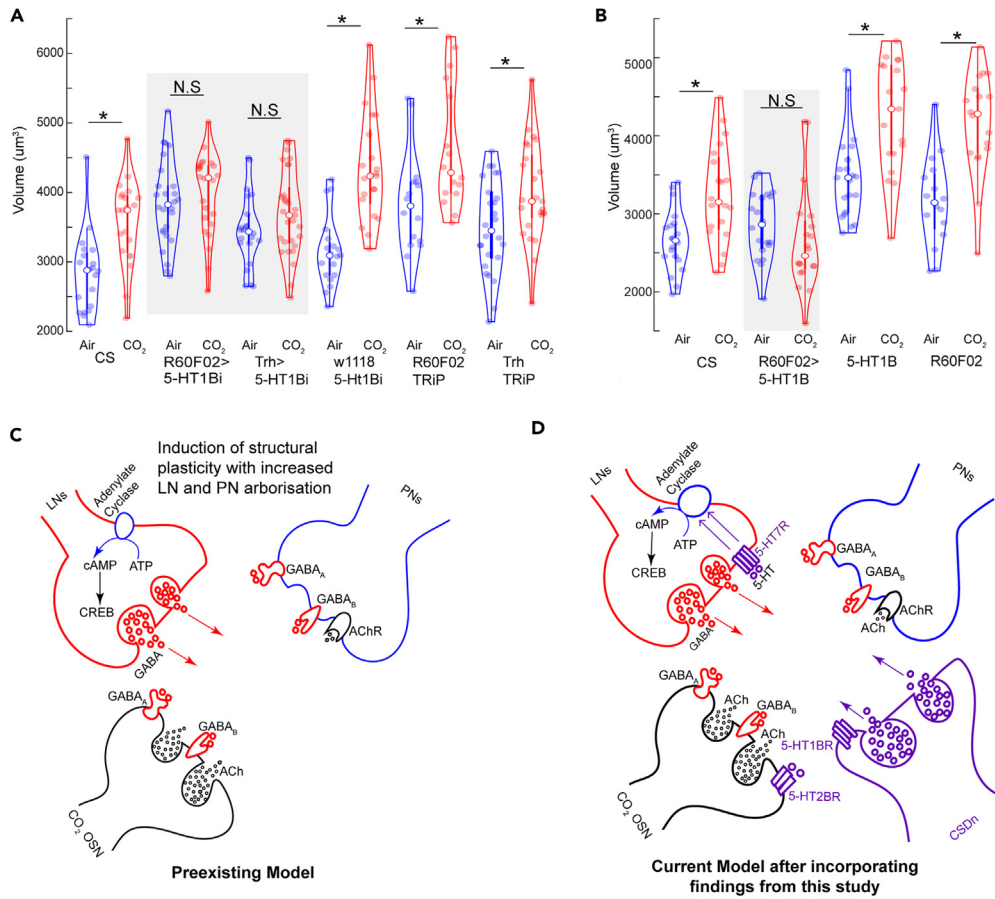


Figure 7. Serotonergic signaling during the critical period

(A) Quantification of V glomerulus volumes comparing air- and 5% CO₂-exposed flies during the critical period. Six genotypes are shown here from left to right: CS (Canton-S wildtype), R60F02>5-HT1Bi (RNAi knockdown in CSDNs), Trh>1Bi (5-HT1B knockdown in all serotonergic cells), w1118,5-HT1Bi (background control for Gal4), R60F02, TRiP (background control for 5-HT1B-RNAi crossed with CSDn line), and Trh, TRiP (background control for 5-HT1B-RNAi crossed with Trh line). (B) Quantification of V glomerulus volumes comparing air- and 5% CO₂-exposed flies during the critical period. Four genotypes are shown here from left to right: CS (Canton-S wildtype), R60F02>5-HT1B (overexpression of 5-HT1B in CSDNs), 5-HT1B (control for UAS), and R60F02 (control for Gal4).

(C) During the critical period, chronic odor exposure leads to OSN-dependent activation of LNs and PN_s. Activation of GABAergic LNs induces GABA release that modulates OSN and PN responses. cAMP-dependent mechanisms in GABAergic LNs lead to CREB-dependent gene transcription that promotes structural plasticity in the LN and PN arbors, resulting in glomerulus-specific volume increase.

(D) Our results (in pink) show 5-HT also plays a role within the existing model of CPP. 5-HT is released from the CSDNs and is tightly regulated by 5-HT1BRs during the critical period. Differential expression of 5-HT2BR neurons on the OSNs regulates structural plasticity in the LNs and PN_s. 5-HT7-mediated GABAergic LN activation interacts with the preexisting model of cAMP-dependent gene transcription to facilitate CPP. GABAergic signaling from the LNs modulate global OSN activation levels during the critical period. * indicates $p < 0.05$; N.S indicates $p > 0.05$. $n \geq 15$, and gray boxes indicate experimental fly lines in all cases. All violin plots include individual data points (colored circles) and mean (white circle). The boxplot of the data is also represented at the center of the violin. Detailed genotypes of flies for each experimental condition can be found in Table 1 and the antibody concentrations used in Table 2.

we showed the effects of 5-HT on the V-glomerulus that increases in size in response to its cognate odor during the critical period. However, there are other glomerulus like the VM7 that shows OSN retraction and a volume decrease in response to odor exposure during the critical period. It will be interesting to note how 5-HT differentially modulates such glomeruli.

RESOURCE AVAILABILITY

Lead contact

Further information and requests for resources and reagents should be directed to and fulfilled by the lead contact, Andrew M. Dacks (amd358@case.edu).

Materials availability

All plasmids and flies generated in this study have been deposited to Addgene and Bloomington Drosophila Stock Center, respectively. The accession number to order these reagents can be found in the key resources table.

Data and code availability

- All raw confocal data are available upon request from the [lead contact](#).
- All codes to plot the figures and analyze data were written in MATLAB and available from the [lead contact](#) upon request.
- Any additional information required to reanalyze the data reported in this paper is available from the [lead contact](#) upon request.

ACKNOWLEDGMENTS

We thank Dr. Eric Horstlick for helpful feedback on the manuscript and Jonathan Schenk and Marryn Bennett for technical guidance. We thank Dr. Ricardo Arendea for hosting parts of these experiments. We also thank Dr. Jing Wang, Dr. Jill Wildonger, Dr. Herman Dierick, and Dr. Benjamin White for providing us with different transgenic flies. This work was supported by National Institutes of Health R21DC018945-01 to Q.G., R01 DC016293 to A.M.D. and Q.G., and NSF IOS 2114775 to A.M.D. We thank A.E. Beaven and the UMD Imaging core facility for confocal imaging. Purchase of the Zeiss LSM 980 Airyscan 2 was supported by Award Number 1S10OD025223-01A1 from the National Institutes of Health.

AUTHOR CONTRIBUTIONS

Conceptualization, A.M., H.L.T., A.M.D., and Q.G.; methodology, H.L.T., A.M.D., and Q.G.; validation, A.M., J.M.E., H.L.T., C.M.J.N., and O.M.C.; formal analysis, A.M., J.M.E., H.L.T., C.M.J.N., and O.M.C.; investigation, A.M., J.M.E., H.L.T., C.M.J.N., and O.M.C.; resources, H.L.T., A.M.D., and Q.G.; data curation, A.M., H.L.T., A.M.D., and Q.G.; writing—original draft, A.M., A.M.D., and Q.G.; writing—review & editing, A.M.D. and Q.G.; visualization, A.M., H.L.T., Q.G., and A.M.D.; supervision, Q.G. and A.M.D.; project administration, Q.G. and A.M.D.; funding acquisition, Q.G. and A.M.D. All authors read and approved the manuscript.

DECLARATION OF INTERESTS

The authors declare no competing interests.

STAR★METHODS

Detailed methods are provided in the online version of this paper and include the following:

- [KEY RESOURCES TABLE](#)
- [EXPERIMENTAL MODEL AND STUDY PARTICIPANT DETAILS](#)
- [METHOD DETAILS](#)
 - Fly rearing and maintenance
 - Selective Serotonin Reuptake Inhibitor (SSRI) Treatment
 - Odor exposure
 - Plasmid preparation for CRISPR/Cas9 knock-in
 - Extraction of genomic DNA
 - Generation of fly lines
 - Immunostaining and confocal imaging
- [QUANTIFICATION AND STATISTICAL ANALYSIS](#)
 - Image analysis

SUPPLEMENTAL INFORMATION

Supplemental information can be found online at <https://doi.org/10.1016/j.isci.2024.111083>.

Received: April 15, 2024

Revised: August 11, 2024

Accepted: September 27, 2024

Published: October 9, 2024

REFERENCES

1. Mallick, A., Dacks, A.M., and Gaudry, Q. (2024). Olfactory Critical Periods: How Odor Exposure Shapes the Developing Brain in Mice and Flies. *Biology* 13, 94. <https://doi.org/10.3390/BIOLOGY13020094>.
2. Reh, R.K., Dias, B.G., Nelson, C.A., Kaufer, D., Werker, J.F., Kolb, B., Levine, J.D., and Hensch, T.K. (2020). Critical period regulation across multiple timescales. *Proc. Natl. Acad. Sci. USA* 117, 23242–23251. <https://doi.org/10.1073/pnas.1820836117>.
3. Hensch, T.K. (2005). Critical period plasticity in local cortical circuits. *Nat. Rev. Neurosci.* 6, 877–888. <https://doi.org/10.1038/nrn1787>.
4. Wang, Y., Gu, Q., and Cynader, M.S. (1997). Blockade of serotonin-2C receptors by mesulergine reduces ocular dominance plasticity in kitten visual cortex. *Exp. Brain Res.* 114, 321–328. <https://doi.org/10.1007/PL00005640>.
5. Gu, Q., and Singer, W. (1995). Involvement of Serotonin in Developmental Plasticity of Kitten Visual Cortex. *Eur. J. Neurosci.* 7, 1146–1153. <https://doi.org/10.1111/j.1460-9568.1995.tb01104.x>.
6. Jitsuki, S., Takemoto, K., Kawasaki, T., Tada, H., Takahashi, A., Becamel, C., Sano, A., Yuzaki, M., Zukin, R.S., Ziff, E.B., et al. (2011). Serotonin Mediates Cross-Modal Reorganization of Cortical Circuits. *Neuron* 69, 780–792. <https://doi.org/10.1016/j.NEURON.2011.01.016>.
7. Dyck, R.H., and Cynader, M.S. (1993). Autoradiographic localization of serotonin receptor subtypes in cat visual cortex: transient regional, laminar, and columnar distributions during postnatal development. *J. Neurosci.* 13, 4316–4338. <https://doi.org/10.1523/JNEUROSCI.13-10-04316.1993>.
8. Teissier, A., Soiza-Reilly, M., and Gaspar, P. (2017). Refining the role of 5-HT in postnatal development of brain circuits. *Front. Cell. Neurosci.* 11, 139. <https://doi.org/10.3389/fncel.2017.00139>.
9. Suri, D., Teixeira, C.M., Cagliostro, M.K.C., Mahadevia, D., and Ansorge, M.S. (2015). Monoamine-Sensitive Developmental Periods Impacting Adult Emotional and Cognitive Behaviors. *Neuropsychopharmacology* 40, 88–112. <https://doi.org/10.1038/npp.2014.231>.
10. Higa, G.S.V., Francis-Oliveira, J., Carlos-Lima, E., Tamais, A.M., Borges, F.d.S., Kihara, A.H., Shieh, I.C., Ulrich, H.,

- Chiavegatto, S., and De Pasquale, R. (2022). 5-HT-dependent synaptic plasticity of the prefrontal cortex in postnatal development. *Sci. Rep.* 12, 21015. <https://doi.org/10.1038/s41598-022-23767-9>.
11. Ogelman, R., Gomez Wulschner, L.E., Hoelscher, V.M., Hwang, I.-W., Chang, V.N., and Oh, W.C. (2024). Serotonin modulates excitatory synapse maturation in the developing prefrontal cortex. *Nat. Commun.* 15, 1368. <https://doi.org/10.1038/s41467-024-45734-w>.
 12. Hildebrand, J.G., and Shepherd, G.M. (1997). Mechanisms of olfactory discrimination: converging evidence for common principles across phyla. *Annu. Rev. Neurosci.* 20, 595–631. <https://doi.org/10.1146/ANNUREV.NEURO.20.1.595>.
 13. Hallem, E.A., and Carlson, J.R. (2006). Coding of Odors by a Receptor Repertoire. *Cell* 125, 143–160. <https://doi.org/10.1016/j.cell.2006.01.050>.
 14. Hallem, E.A., Ho, M.G., and Carlson, J.R. (2004). The molecular basis of odor coding in the *Drosophila* antenna. *Cell* 117, 965–979. <https://doi.org/10.1016/j.cell.2004.05.012>.
 15. Benton, R., Sachse, S., Michnick, S.W., and Vosshall, L.B. (2006). Atypical membrane topology and heteromeric function of *Drosophila* odorant receptors in vivo. *PLoS Biol.* 4, e20. <https://doi.org/10.1371/JOURNAL.PBIO.0040020>.
 16. Benton, R., Vannice, K.S., Gomez-Diaz, C., and Vosshall, L.B. (2009). Variant Ionotropic Glutamate Receptors as Chemosensory Receptors in *Drosophila*. *Cell* 136, 149–162. <https://doi.org/10.1016/j.cell.2008.12.001>.
 17. Wilson, R.I. (2013). Early Olfactory Processing in *Drosophila*: Mechanisms and Principles. *Annu. Rev. Neurosci.* 36, 217–241. <https://doi.org/10.1146/annurev-neuro-062111-150533>.
 18. Fabian, B., and Sachse, S. (2023). Experience-dependent plasticity in the olfactory system of *Drosophila melanogaster* and other insects. *Front. Cell. Neurosci.* 17, 1130091. <https://doi.org/10.3389/fncel.2023.1130091>.
 19. Fabian, B., Grabe, V., Beutel, R.G., Hansson, B.S., and Sachse, S. (2023). Experience-dependent plasticity of a highly specific olfactory circuit in *Drosophila melanogaster*. Preprint at bioRxiv. <https://doi.org/10.1101/2023.07.26.550642>.
 20. Das, S., Sadanandappa, M.K., Dervan, A., Larkin, A., Lee, J.A., Sudhakaran, I.P., Priya, R., Heidari, R., Holohan, E.E., Pimentel, A., et al. (2011). Plasticity of local GABAergic interneurons drives olfactory habituation. *Proc. Natl. Acad. Sci. USA* 108, E646–E654. <https://doi.org/10.1073/pnas.1106411108>.
 21. Chodankar, A., Sadanandappa, M.K., Raghavan, K.V., and Ramaswami, M. (2020). Glomerulus-Selective regulation of a critical period for interneuron plasticity in the *drosophila* antennal lobe. *J. Neurosci.* 40, 5549–5560. <https://doi.org/10.1523/JNEUROSCI.2192-19.2020>.
 22. Golovin, R.M., Vest, J., and Broadie, K. (2021). Neuron-specific FMRP roles in experience-dependent remodeling of olfactory brain innervation during an early-life critical period. *J. Neurosci.* 41, 1218–1241. <https://doi.org/10.1523/JNEUROSCI.2167-20.2020>.
 23. Golovin, R.M., Vest, J., Vita, D.J., and Broadie, K. (2019). Activity-dependent remodeling of *Drosophila* olfactory sensory neuron brain innervation during an early-life critical period. *J. Neurosci.* 39, 2995–3012. <https://doi.org/10.1523/JNEUROSCI.2223-18.2019>.
 24. Kidd, S., and Lieber, T. (2016). Mechanism of Notch Pathway Activation and Its Role in the Regulation of Olfactory Plasticity in *Drosophila melanogaster*. *PLoS One* 11, e0151279. <https://doi.org/10.1371/journal.pone.0151279>.
 25. Kidd, S., Struhl, G., and Lieber, T. (2015). Notch Is Required in Adult *Drosophila* Sensory Neurons for Morphological and Functional Plasticity of the Olfactory Circuit. *PLoS Genet.* 11, e1005244. <https://doi.org/10.1371/journal.pgen.1005244>.
 26. Lieber, T., Kidd, S., and Struhl, G. (2011). DSL-Notch Signaling in the *Drosophila* Brain in Response to Olfactory Stimulation. *Neuron* 69, 468–481. <https://doi.org/10.1016/j.neuron.2010.12.015>.
 27. Sachse, S., Rueckert, E., Keller, A., Okada, R., Tanaka, N.K., Ito, K., and Vosshall, L.B. (2007). Activity-Dependent Plasticity in an Olfactory Circuit. *Neuron* 56, 838–850. <https://doi.org/10.1016/j.neuron.2007.10.035>.
 28. Hensch, T.K., and Quinlan, E.M. (2018). Critical periods in amblyopia. *Vis. Neurosci.* 35, E014. <https://doi.org/10.1017/S0952523817000219>.
 29. Takesian, A.E., Bogart, L.J., Lichtman, J.W., and Hensch, T.K. (2018). Inhibitory circuit gating of auditory critical-period plasticity. *Nat. Neurosci.* 21, 218–227. <https://doi.org/10.1038/s41593-017-0064-2>.
 30. Toyozumi, T., Miyamoto, H., Yazaki-Sugiyama, Y., Atapour, N., Hensch, T.K., and Miller, K.D. (2013). A Theory of the Transition to Critical Period Plasticity: Inhibition Selectively Suppresses Spontaneous Activity. *Neuron* 80, 51–63.
 31. Berardi, N., Pizzorusso, T., Ratto, G.M., and Maffei, L. (2003). Molecular basis of plasticity in the visual cortex. *Trends Neurosci.* 26, 369–378. [https://doi.org/10.1016/S0166-2236\(03\)00168-1](https://doi.org/10.1016/S0166-2236(03)00168-1).
 32. Kirkwood, A. (2000). Serotonergic control of developmental plasticity. *Proc. Natl. Acad. Sci. USA* 97, 1951–1952. <https://doi.org/10.1073/pnas.070044697>.
 33. Kojic, L., Dyck, R.H., Gu, Q., Douglas, R.M., Matsubara, J., and Cynader, M.S. (2000). Columnar distribution of serotonin-dependent plasticity within kitten striate cortex. *Proc. Natl. Acad. Sci. USA* 97, 1841–1844. <https://doi.org/10.1073/pnas.97.4.1841>.
 34. Maya Vetencourt, J.F., Tiraboschi, E., Spolidoro, M., Castrén, E., and Maffei, L. (2011). Serotonin triggers a transient epigenetic mechanism that reinstates adult visual cortex plasticity in rats. *Eur. J. Neurosci.* 33, 49–57. <https://doi.org/10.1111/j.1460-9568.2010.07488.x>.
 35. Vetencourt, J.F.M., Sale, A., Viegi, A., Baroncelli, L., De Pasquale, R., O’Leary, O.F., Castrén, E., and Maffei, L. (2008). The antidepressant fluoxetine restores plasticity in the adult visual cortex. *Science* 320, 385–388. <https://doi.org/10.1126/SCIENCE.1150516>.
 36. Suh, G.S.B., Wong, A.M., Hergarden, A.C., Wang, J.W., Simon, A.F., Benzer, S., Axel, R., and Anderson, D.J. (2004). A single population of olfactory sensory neurons mediates an innate avoidance behaviour in *Drosophila*. *Nature* 431, 854–859. <https://doi.org/10.1038/nature02980>.
 37. Faucher, C., Forstreuter, M., Hilker, M., and De Bruyne, M. (2006). Behavioral responses of *Drosophila* to biogenic levels of carbon dioxide depend on life-stage, sex and olfactory context. *J. Exp. Biol.* 209, 2739–2748. <https://doi.org/10.1242/JEB.02297>.
 38. Coates, K.E., Majot, A.T., Zhang, X., Michael, C.T., Spitzer, S.L., Gaudry, Q., and Dacks, A.M. (2017). Identified Serotonergic Modulatory Neurons Have Heterogeneous Synaptic Connectivity within the Olfactory System of *Drosophila*. *J. Neurosci.* 37, 7318–7331. <https://doi.org/10.1523/JNEUROSCI.0192-17.2017>.
 39. Dacks, A.M., Christensen, T.A., and Hildebrand, J.G. (2006). Phylogeny of a serotonin-immunoreactive neuron in the primary olfactory center of the insect brain. *J. Comp. Neurol.* 498, 727–746. <https://doi.org/10.1002/CNE.21076>.
 40. Coates, K.E., Calle-Schuler, S.A., Helmick, L.M., Knotts, V.L., Martik, B.N., Salman, F., Warner, L.T., Valla, S.V., Bock, D.D., and Dacks, A.M. (2020). The Wiring Logic of an Identified Serotonergic Neuron That Spans Sensory Networks. *J. Neurosci.* 40, 6309–6327. <https://doi.org/10.1523/JNEUROSCI.0552-20.2020>.
 41. Zhang, X., and Gaudry, Q. (2016). Functional integration of a serotonergic neuron in the *drosophila* antennal lobe. *Elife* 5, e16836. <https://doi.org/10.7554/eLife.16836>.
 42. Sun, X.J., Tolbert, L.P., and Hildebrand, J.G. (1993). Ramification pattern and ultrastructural characteristics of the serotonin-immunoreactive neuron in the antennal lobe of the moth *Manduca sexta*: A laser scanning confocal and electron microscopic study. *J. Comp. Neurol.* 338, 5–16. <https://doi.org/10.1002/CNE.903380103>.
 43. Jenett, A., Rubin, G.M., Ngo, T.T.B., Shepherd, D., Murphy, C., Dionne, H., Pfeiffer, B.D., Cavallaro, A., Hall, D., Jeter, J., et al. (2012). A GAL4-Driver Line Resource for *Drosophila* Neurobiology. *Cell Rep.* 2, 991–1001. <https://doi.org/10.1016/j.celrep.2012.09.011>.
 44. Suzuki, Y., Schenk, J.E., Tan, H., and Gaudry, Q. (2020). A Population of Interneurons Signals Changes in the Basal Concentration of Serotonin and Mediates Gain Control in the *Drosophila* Antennal Lobe. *Curr. Biol.* 30, 1110–1118.e4. <https://doi.org/10.1016/j.cub.2020.01.018>.
 45. Erber, J., Kloppenburg, P., and Scheidler, A. (1993). Neuromodulation by serotonin and octopamine in the honeybee: behaviour, neuroanatomy and electrophysiology. *Experientia* 49, 1073–1083. <https://doi.org/10.1007/BF01929916>.
 46. Bessonova, Y., and Raman, B. (2024). Serotonergic amplification of odor-evoked neural responses maps onto flexible behavioral outcomes. *Elife* 12. <https://doi.org/10.7554/ELIFE.91890.2>.
 47. Dacks, A.M., Christensen, T.A., and Hildebrand, J.G. (2008). Modulation of olfactory information processing in the antennal lobe of *Manduca sexta* by serotonin. *J. Neurophysiol.* 99, 2077–2085. <https://doi.org/10.1152/JN.01372.2007>.
 48. Gatellier, L., Nagao, T., and Kanzaki, R. (2004). Serotonin modifies the sensitivity of the male silkworm to pheromone. *J. Exp. Biol.* 207, 2487–2496. <https://doi.org/10.1242/JEB.01035>.
 49. Kloppenburg, P., Ferns, D., and Mercer, A.R. (1999). Serotonin Enhances Central

- Olfactory Neuron Responses to Female Sex Pheromone in the Male Sphinx Moth *Manduca sexta*. *J. Neurosci.* 19, 8172–8181. <https://doi.org/10.1523/JNEUROSCI.19-19-08172.1999>.
50. Dunham, K.E., and Venton, B.J. (2022). SSRI antidepressants differentially modulate serotonin reuptake and release in *Drosophila*. *J. Neurochem.* 162, 404–416. <https://doi.org/10.1111/JNC.15658>.
51. Witz, P., Amlaiky, N., Plassat, J.L., Maroteaux, L., Borrelli, E., and Hen, R. (1990). Cloning and characterization of a *Drosophila* serotonin receptor that activates adenylate cyclase. *Proc. Natl. Acad. Sci. USA* 87, 8940–8944. <https://doi.org/10.1073/PNAS.87.22.8940>.
52. Saudou, F., Boschert, U., Amlaiky, N., Plassat, J.-L., and Hen, R. (1992). A family of *Drosophila* serotonin receptors with distinct intracellular signalling properties and expression patterns. *EMBO J.* 11, 7–17. <https://doi.org/10.1002/J.1460-2075.1992.TB05021.X>.
53. Colas, J.F., Launay, J.M., Kellermann, O., Rosay, P., and Maroteaux, L. (1995). *Drosophila* 5-HT2 serotonin receptor: coexpression with fushi tarazu during segmentation. *Proc. Natl. Acad. Sci. USA* 92, 5441–5445. <https://doi.org/10.1073/PNAS.92.12.5441>.
54. Qian, Y., Cao, Y., Deng, B., Yang, G., Li, J., Xu, R., Zhang, D., Huang, J., and Rao, Y. (2017). Sleep homeostasis regulated by 5HT2b receptor in a small subset of neurons in the dorsal fan-shaped body of *Drosophila*. *Elife* 6, e26519. <https://doi.org/10.7554/Elife.26519>.
55. Gnerer, J.P., Venken, K.J.T., and Dierick, H.A. (2015). Gene-specific cell labeling using MiMIC transposons. *Nucleic Acids Res.* 43, e56. <https://doi.org/10.1093/NAR/GKV113>.
56. Cheung, U.S., Shayan, A.J., Boulianne, G.L., and Atwood, H.L. (1999). *Drosophila* larval neuromuscular junction's responses to reduction of cAMP in the nervous system. *J. Neurobiol.* 40, 1–13. [https://doi.org/10.1002/\(SICI\)1097-4695\(199907\)40:1%3C1::AID-NEU1%3E3.0.CO;2-1](https://doi.org/10.1002/(SICI)1097-4695(199907)40:1%3C1::AID-NEU1%3E3.0.CO;2-1).
57. Root, C.M., Masuyama, K., Green, D.S., Enell, L.E., Nässel, D.R., Lee, C.H., and Wang, J.W. (2008). A Presynaptic Gain Control Mechanism Fine-Tunes Olfactory Behavior. *Neuron* 59, 311–321. <https://doi.org/10.1016/J.NEURON.2008.07.003>.
58. Franco, L.M., Okray, Z., Linneweber, G.A., Hassan, B.A., and Yaksi, E. (2017). Reduced Lateral Inhibition Impairs Olfactory Computations and Behaviors in a *Drosophila* Model of Fragile X Syndrome. *Curr. Biol.* 27, 1111–1123. <https://doi.org/10.1016/j.cub.2017.02.065>.
59. Rotelli, M.D., Bolling, A.M., Killion, A.W., Weinberg, A.J., Dixon, M.J., and Calvi, B.R. (2019). An RNAi Screen for Genes Required for Growth of *Drosophila* Wing Tissue. *G3 (Bethesda)* 9, 3087–3100. <https://doi.org/10.1534/G3.119.400581>.
60. Sizemore, T.R., and Dacks, A.M. (2016). Serotonergic Modulation Differentially Targets Distinct Network Elements within the Antennal Lobe of *Drosophila melanogaster*. *Sci. Rep.* 6, 37119. <https://doi.org/10.1038/srep37119>.
61. Bonanno, S.L., Sanfilippo, P., Eamani, A., Sampson, M.M., Kandagedon, B., Li, K., Burns, G.D., Makar, M.E., Zipursky, S.L., and Krantz, D.E. (2024). Constitutive and conditional epitope-tagging of endogenous G protein coupled receptors in *Drosophila*. *J. Neurosci.* 44, e2377232024. <https://doi.org/10.1523/JNEUROSCI.2377-23.2024>.
62. Vicario, M., Cieri, D., Vallesse, F., Catoni, C., Barazzuol, L., Berto, P., Grinzato, A., Barbieri, L., Brini, M., and Cali, T. (2019). A split-GFP tool reveals differences in the mitochondrial distribution of wt and mutant alpha-synuclein. *Cell Death Dis.* 10, 857. <https://doi.org/10.1038/s41419-019-2092-1>.
63. Pedelacq, J.D., and Cabantous, S. (2019). Development and Applications of Superfolder and Split Fluorescent Protein Detection Systems in Biology. *Int. J. Mol. Sci.* 20, 3479. <https://doi.org/10.3390/IJMS20143479>.
64. Kamiyama, R., Banzai, K., Liu, P., Marar, A., Tamura, R., Jiang, F., Fitch, M.A., Xie, J., and Kamiyama, D. (2021). Cell-type-specific, multicolor labeling of endogenous proteins with split fluorescent protein tags in *Drosophila*. *Proc. Natl. Acad. Sci. USA* 118, e2024690118. <https://doi.org/10.1073/PNAS.2024690118>.
65. Ran, F.A., Hsu, P.D., Wright, J., Agarwala, V., Scott, D.A., and Zhang, F. (2013). Genome engineering using the CRISPR-Cas9 system. *Nat. Protoc.* 8, 2281–2308. <https://doi.org/10.1038/nprot.2013.143>.
66. Gratz, S.J., Ukken, F.P., Rubinstein, C.D., Thiede, G., Donohue, L.K., Cummings, A.M., and Oconnor-Giles, K.M. (2014). Highly specific and efficient CRISPR/Cas9-catalyzed homology-directed repair in *Drosophila*. *Genetics* 196, 961–971. <https://doi.org/10.1534/GENETICS.113.160713>.
67. Cabantous, S., Terwilliger, T.C., and Waldo, G.S. (2005). Protein tagging and detection with engineered self-assembling fragments of green fluorescent protein. *Nat. Biotechnol.* 23, 102–107. <https://doi.org/10.1038/nbt1044>.
68. Romei, M.G., and Boxer, S.G. (2019). Split Green Fluorescent Proteins: Scope, Limitations, and Outlook. *Annu. Rev. Biophys.* 48, 19–44. <https://doi.org/10.1146/annurev-biophys-051013-022846>.
69. Sizemore, T.R., Hurler, L.M., and Dacks, A.M. (2020). Serotonergic modulation across sensory modalities. *J. Neurophysiol.* 123, 2406–2425. <https://doi.org/10.1152/JN.00034.2020>.
70. Kwon, J.Y., Dahanukar, A., Weiss, L.A., and Carlson, J.R. (2007). The molecular basis of CO2 reception in *Drosophila*. *Proc. Natl. Acad. Sci. USA* 104, 3574–3578. <https://doi.org/10.1073/PNAS.0700079104>.
71. Tiger, M., Varnäs, K., Okubo, Y., and Lundberg, J. (2018). The 5-HT 1B receptor - a potential target for antidepressant treatment. *Psychopharmacology (Berl)* 235, 1317–1334. <https://doi.org/10.1007/S00213-018-4872-1>.
72. Middlemiss, D.N., and Hutson, P.H. (1990). The 5-HT1B Receptors. *Ann. N. Y. Acad. Sci.* 600, 132–148. <https://doi.org/10.1111/J.1749-6632.1990.TB16878.X>.
73. Brazell, M.P., Marsden, C.A., Nisbet, A.P., and Routledge, C. (1985). The 5-HT1 receptor agonist RU-24969 decreases 5-hydroxytryptamine (5-HT) release and metabolism in the rat frontal cortex *in vitro* and *in vivo*. *Br. J. Pharmacol.* 86, 209–216. <https://doi.org/10.1111/J.1476-5381.1985.TB09451.X>.
74. Barnes, N.M., and Sharp, T. (1999). A review of central 5-HT receptors and their function. *Neuropharmacology* 38, 1083–1152. [https://doi.org/10.1016/S0028-3908\(99\)00010-6](https://doi.org/10.1016/S0028-3908(99)00010-6).
75. Hagan, C.E., Mcdevitt, R.A., Liu, Y., Furay, A.R., and Neumaier, J.F. (2012). 5-HT1B autoreceptor regulation of serotonin transporter activity in synaptosomes. *Synapse* 66, 1024–1034. <https://doi.org/10.1002/SYN.21608>.
76. Larsen, B., Cui, Z., Adebimpe, A., Pines, A., Alexander-Bloch, A., Bertolero, M., Calkins, M.E., Gur, R.E., Gur, R.C., Mahadevan, A.S., et al. (2022). A developmental reduction of the excitation:inhibition ratio in association cortex during adolescence. *Sci. Adv.* 8, 8750. <https://doi.org/10.1126/sciadv.abj8750>.
77. Levelt, C.N., and Hübener, M. (2012). Critical-period plasticity in the visual cortex. *Annu. Rev. Neurosci.* 35, 309–330. <https://doi.org/10.1146/annurev-neuro-061010-113813>.
78. Erzurumlu, R.S., and Gaspar, P. (2012). Development and critical period plasticity of the barrel cortex. *Eur. J. Neurosci.* 35, 1540–1553. <https://doi.org/10.1111/J.1460-9568.2012.08075.X>.
79. Olsen, S.R., and Wilson, R.I. (2008). Lateral presynaptic inhibition mediates gain control in an olfactory circuit. *Nature* 452, 956–960. <https://doi.org/10.1038/nature06864>.
80. Yaksi, E., and Wilson, R.I. (2010). Electrical Coupling between Olfactory Glomeruli. *Neuron* 67, 1034–1047. <https://doi.org/10.1016/j.neuron.2010.08.041>.
81. Nagel, K.I., Wilson, R.I., Nagel, K.I., and Wilson, R.I. (2011). Biophysical mechanisms underlying olfactory receptor neuron dynamics. *Nat. Neurosci.* 14, 208–218. <https://doi.org/10.1038/nn.2725>.
82. Liu, W.W., and Wilson, R.I. (2013). Glutamate is an inhibitory neurotransmitter in the *Drosophila* olfactory system. *Proc. Natl. Acad. Sci. USA* 110, 10294–10299. <https://doi.org/10.1073/PNAS.1220560110>.
83. Hong, E.J., and Wilson, R.I. (2015). Simultaneous encoding of odors by channels with diverse sensitivity to inhibition. *Neuron* 85, 573–589. <https://doi.org/10.1016/j.neuron.2014.12.040>.
84. Nagel, K.I., Hong, E.J., and Wilson, R.I. (2015). Synaptic and circuit mechanisms promoting broadband transmission of olfactory stimulus dynamics. *Nat. Neurosci.* 18, 56–65. <https://doi.org/10.1038/nn.3895>.
85. Gervasi, N., Tchénio, P., and Preat, T. (2010). PKA Dynamics in a *Drosophila* Learning Center: Coincidence Detection by Rutabaga Adenyllyl Cyclase and Spatial Regulation by Dunce Phosphodiesterase. *Neuron* 65, 516–529. <https://doi.org/10.1016/j.neuron.2010.01.014>.
86. Stam, N.J., Roesink, C., Dijkcs, F., Garritsen, A., Van Herpen, A., and Olive, W. (1997). Human serotonin 5-HT7 receptor: cloning and pharmacological characterisation of two receptor variants. *FEBS Lett.* 413, 489–494. [https://doi.org/10.1016/S0014-5793\(97\)00964-2](https://doi.org/10.1016/S0014-5793(97)00964-2).
87. Hobson, R.J., Hapiak, V.M., Xiao, H., Buehrer, K.L., Komuniecki, P.R., and Komuniecki, R.W. (2006). SER-7, a *Caenorhabditis elegans* 5-HT7-like Receptor, Is Essential for the 5-HT Stimulation of Pharyngeal Pumping and Egg Laying. *Genetics* 172, 159–169. <https://doi.org/10.1534/GENETICS.105.044495>.
88. Omar, M., Zhou, Y., Planting, E., Parvataneni, R., and Hung, S. (2009). Combined active triangulation, morphology

- scheme for active shape retrieval. *Sens. Rev.* 29, 233–239. <https://doi.org/10.1108/02602280910967648>.
89. Shen, Y., Monsma, F.J., Metcalf, M.A., Jose, P.A., Hamblin, M.W., and Sibley, D.R. (1993). Molecular cloning and expression of a 5-hydroxytryptamine₇ serotonin receptor subtype. *J. Biol. Chem.* 268, 18200–18204. [https://doi.org/10.1016/S0021-9258\(17\)46830-X](https://doi.org/10.1016/S0021-9258(17)46830-X).
 90. Ruat, M., Traffort, E., Leurs, R., Tardivel-Lacombe, J., Diaz, J., Arrang, J.M., and Schwartz, J.C. (1993). Molecular cloning, characterization, and localization of a high-affinity serotonin receptor (5-HT₇) activating cAMP formation. *Proc. Natl. Acad. Sci. USA* 90, 8547–8551. <https://doi.org/10.1073/PNAS.90.18.8547>.
 91. Qi, Y.X., Jin, M., Ni, X.Y., Ye, G.Y., Lee, Y., and Huang, J. (2017). Characterization of three serotonin receptors from the small white butterfly, *Pieris rapae*. *Insect Biochem. Mol. Biol.* 87, 107–116. <https://doi.org/10.1016/J.IBMB.2017.06.011>.
 92. Dacks, A.M., Reale, V., Pi, Y., Zhang, W., Dacks, J.B., Nighorn, A.J., and Evans, P.D. (2013). A Characterization of the *Manduca sexta* Serotonin Receptors in the Context of Olfactory Neuromodulation. *PLoS One* 8, e69422. <https://doi.org/10.1371/JOURNAL.PONE.0069422>.
 93. Schlenstedt, J., Balfanz, S., Baumann, A., and Blenau, W. (2006). Am5-HT₇: molecular and pharmacological characterization of the first serotonin receptor of the honeybee (*Apis mellifera*). *J. Neurochem.* 98, 1985–1998. <https://doi.org/10.1111/J.1471-4159.2006.04012.X>.
 94. Pietrantonio, P.V., Jagge, C., and McDowell, C. (2001). Cloning and expression analysis of a 5HT₇-like serotonin receptor cDNA from mosquito *Aedes aegypti* female excretory and respiratory systems. *Insect Mol. Biol.* 10, 357–369. <https://doi.org/10.1046/J.0962-1075.2001.00274.X>.
 95. Röser, C., Jordan, N., Balfanz, S., Baumann, A., Walz, B., Baumann, O., and Blenau, W. (2012). Molecular and Pharmacological Characterization of Serotonin 5-HT_{2α} and 5-HT₇ Receptors in the Salivary Glands of the Blowfly *Calliphora vicina*. *PLoS One* 7, e49459. <https://doi.org/10.1371/JOURNAL.PONE.0049459>.
 96. Lee, D.W., and Pietrantonio, P.V. (2003). In vitro expression and pharmacology of the 5-HT₇-like receptor present in the mosquito *Aedes aegypti* tracheolar cells and hindgut-associated nerves. *Insect Mol. Biol.* 12, 561–569. <https://doi.org/10.1046/J.1365-2583.2003.00441.X>.
 97. Vleugels, R., Lenaerts, C., Vanden Broeck, J., and Verlinden, H. (2014). Signalling properties and pharmacology of a 5-HT₇-type serotonin receptor from *Tribolium castaneum*. *Insect Mol. Biol.* 23, 230–243. <https://doi.org/10.1111/IMB.12076>.
 98. Hensch, T.K., and Fagiolini, M. (2005). Excitatory–inhibitory balance and critical period plasticity in developing visual cortex. *Prog. Brain Res.* 147, 115–124. [https://doi.org/10.1016/S0079-6123\(04\)47009-5](https://doi.org/10.1016/S0079-6123(04)47009-5).
 99. Hunter, I., Coulson, B., Pettini, T., Davies, J.J., Parkin, J., Landgraf, M., and Baines, R.A. (2024). Balance of activity during a critical period tunes a developing network. *Elife* 12. <https://doi.org/10.7554/ELIFE.91599>.
 100. Carlos-Lima, E., Higa, G.S.V., Viana, F.J.C., Tamais, A.M., Cruvinel, E., Borges, F.d.S., Francis-Oliveira, J., Ulrich, H., and De Pasquale, R. (2023). Serotonergic Modulation of the Excitation/Inhibition Balance in the Visual Cortex. *Int. J. Mol. Sci.* 25, 519. <https://doi.org/10.3390/IJMS25010519>.
 101. Kayser, M.S., Yue, Z., and Sehgal, A. (2014). A Critical Period of Sleep for Development of Courtship Circuitry and Behavior in *Drosophila*. *Science* 344, 269–274. <https://doi.org/10.1126/SCIENCE.1250553>.
 102. Kaneko, T., Macara, A.M., Li, R., Hu, Y., Iwasaki, K., Dunning, Z., Firestone, E., Horvatic, S., Guntur, A., Shafer, O.T., et al. (2017). Serotonergic Modulation Enables Pathway-Specific Plasticity in a Developing Sensory Circuit in *Drosophila*. *Neuron* 95, 623–638.e4. <https://doi.org/10.1016/j.neuron.2017.06.034>.
 103. Schenk, J.E., and Gaudry, Q. (2023). Nonspiking Interneurons in the *Drosophila* Antennal Lobe Exhibit Spatially Restricted Activity. *eNeuro* 10, ENEURO.0109-22.2022. <https://doi.org/10.1523/ENEURO.0109-22.2022>.
 104. Bonanno, S.L., and Krantz, D.E. (2023). Transcriptional changes in specific subsets of *Drosophila* neurons following inhibition of the serotonin transporter. *Transl. Psychiatry* 13, 226. <https://doi.org/10.1038/s41398-023-02521-3>.
 105. Ostrovsky, A., Cachero, S., and Jefferis, G. (2013). Clonal Analysis of Olfaction in *Drosophila*: Immunocytochemistry and Imaging of Fly Brains. *Cold Spring Harb. Protoc.* 2013, 342–346. <https://doi.org/10.1101/pdb.prot071720>.
 106. Legland, D., Arganda-Carreras, I., and Andrey, P. (2016). MorphoLibJ: Integrated library and plugins for mathematical morphology with ImageJ. *Bioinformatics* 32, 3532–3534. <https://doi.org/10.1093/BIOINFORMATICS/BTW413>.
 107. Fitzpatrick, M. (2014). Measuring cell fluorescence using ImageJ. Github. <https://github.com/mfitzp/theolb/blob/master/imaging/measuring-cell-fluorescence-using-imagej.rst>.

STAR★METHODS

KEY RESOURCES TABLE

REAGENT or RESOURCE	SOURCE	IDENTIFIER
Antibodies		
anti-hemagglutinin (HA)	Thermo Fisher Scientific	26183; RRID: AB_2533049
anti-5-HT	Immunostar	20080; RRID: AB_572263
anti-reconstituted GFP	Sigma	G6539; RRID: AB_259941
anti-GFP	Abcam	ab13970 ; RRID: AB_300798
anti-Bruchpilot	Developmental Studies Hybridoma Bank (DSHB)	nc82; RRID: AB_2314866
anti-N-Cadherin (n-cad)	Developmental Studies Hybridoma Bank (DSHB)	DN-Ex #8; RRID: AB_528121
anti-chicken Alexa Fluor 488	Thermo Fisher Scientific	A-11039; RRID: AB_2534096
anti-mouse Alexa Fluor 488	Thermo Fisher Scientific	A-11004; RRID: AB_2534072
anti-rabbit Alexa Fluor 546	Thermo Fisher Scientific	A-10040; RRID: AB_2534016
anti-mouse Alexa Fluor 633	Thermo Fisher Scientific	A-21050; RRID: AB_2535718
Bacterial and virus strains		
DH5 α competent cells	Thermo Fisher Scientific	EC0112
Chemicals, peptides, and recombinant proteins		
Ampicillin	Thermo Fisher Scientific	J60977.06
Fluoxetine Hydrochloride	Sigma Aldrich	56296-78-7
Escitalopram Oxalate	Sigma Aldrich	219861-08-2
Triton-X 100	Thermo Fisher Scientific	A16046.AE
Formaldehyde	Sigma Aldrich	252549
Normal Goat Serum	Thermo Fisher Scientific	PCN5000
Vectashield Antifade Mounting Medium	Vector Laboratories	H-1000-10
Tris-Cl	Invitrogen	15568025
NaCl	Sigma Aldrich	S3014
EDTA	Sigma Aldrich	M5755
Proteinase K	Thermo Fisher Scientific	25530049
Critical commercial assays		
Rapid DNA Ligation Kit	Thermo Fisher Scientific	K1422
NucleoSpin Plasmid Mini kit	Macherey-Nagel	740588.250
pTwist Amp	Twist Bioscience HQ, CA	
Experimental models: Organisms/strains		
Gr21a-Mmus\Cd8a.GFP	Bloomington Drosophila Stock Center (BDSC)	52619
R60F02-Gal4	BDSC	48228
10x-UAS-IVS-mCD8::GFP	BDSC	32185
UAS-Vmat-RNAi	BDSC	44471
Canton-S	BDSC	64349
w1118	BDSC	5905
P{y[+7.7]=CaryP}attP2	BDSC	36303
TI{GAL4}5-HT1A[Gal4] / TI{GAL4}5-HT1A [Gal4]	BDSC	86275
TI{GAL4}5-HT1B[Gal4]/ TI{GAL4}5-HT1B [Gal4]	BDSC	86276
TI{GAL4}5-HT2A[Gal4]/ TI{GAL4}5-HT2A [Gal4]	BDSC	86277
UAS-5-HT2B-RNAi	BDSC	60488

(Continued on next page)

Continued

REAGENT or RESOURCE	SOURCE	IDENTIFIER
Tl{GAL4}5-HT2B{Gal4}/TM3, Sb[1]	BDSC	86278
P{y[+t7.7]=CaryP{attp40}}	BDSC	36304
Tl{GAL4}5-HT7{Gal4}	BDSC	86279
5-HT1A-7×GFP ₁₁ -HA	This study. BDSC	605059
5-HT1A-(MI1140)-T2A-GAL4	Gift from Dr. Herman A. Dierick	
10×UAS-mCD8-GFP	BDSC	32189
MiMIC 5213 HT1B T2A Gal4	Gift from Dr. Herman A. Dierick	
5-HT1B-7×GFP ₁₁ -HA	This study. BDSC	605060
10×UAS-mCD8-GFP	BDSC	32186
5-HT2A-(MI459)-T2A-Gal4	Gift from Dr. Herman A. Dierick	
5-HT2A(BFH)-7×GFP ₁₁ -HA/TM6B, Tb[1]	This study. BDSC.	605061
5-HT2B-(MI6500)-T2A-Gal4	Gift from Dr. Herman A. Dierick	
5-HT2B-7×GFP ₁₁ -HA	This study. BDSC.	605063
5-HT7-(MI215)-T2A-Gal4	Gift from Dr. Herman A. Dierick	
5-HT7-7×GFP ₁₁ -HA	This study. BDSC.	605066
GMR70A09-GAL4	BDSC	47720
10xUAS-sfGFP1-10 (VK00027)	Gift from Dr. Jill Wildonger	BDSC# 93189
NP1227-Gal4 also known as LN1-Gal4	Drosophila Genomics Resource Center (DGRC)	103945
10XQUAS-6XmCherry-HA	BDSC	52269
GMR70A09Q	Dr. Quentin Gaudry. Suzuki et al., 2020	
NP2426-Gal4 also known as LN2-Gal4	DGRC	104198
UAS-mCherry	BDSC	59021
QUAS-mCD8-GFP	BDSC	30002
UAS-5HT7-RNAi	BDSC	32471
P{y[+t7.7] =CaryP}attp2	BDSC	36303
w, UAS-dunce; +; +	Gift from Dr. Benjamin White	
UAS-GABA _B -RNAi; UAS-GABA _B -RNAi	Gift from Dr. Jing Wang	
Peb-Gal4	BDSC	80570
UAS-Rdl-RNAi	BDSC	52903
Orco-Gal4	BDSC	26818
Gr21a-Gal4	BDSC	23890
Gr63a-Gal4	BDSC	9943
UAS-5-HT1B-RNAi	BDSC	51842
Trh-T2A-Gal4	BDSC	84694
UAS-5-HT1B	BDSC	27632
5-HT7-Gal4	Gift from Dr. Charles D. Nichols	
MZ19-Gal4	BDSC	34497
Or56a-Gal4	BDSC	23896
Or23a-Gal4	BDSC	9956
Or47a-Gal4	BDSC	9982
Or13a-Gal4	BDSC	9945
Or67c-Gal4	BDSC	24856
Or67d-Gal4	BDSC	23906

(Continued on next page)

Continued

REAGENT or RESOURCE	SOURCE	IDENTIFIER
<i>Oligonucleotides</i>		
gRNA sequence for CRISPR/Cas9 knock-in of 7×GFP11-HA into 5-HT1A: gaccagtccactaccgcagc	Eurofins Genomics	N.A.
gRNA1 sequence for CRISPR/Cas9 knock-in of 7×GFP11-HA into 5-HT1B: aatttcgacggcgcttcaag	Eurofins Genomics	N.A.
gRNA2 sequence for CRISPR/Cas9 knock-in of 7×GFP11-HA into 5-HT1B: gaaaatttgattcaactga	Eurofins Genomics	N.A.
gRNA1 sequence for CRISPR/Cas9 knock-in of 7×GFP11-HA into 5-HT2A isoform A: catattcaatgcacgttcc	Eurofins Genomics	N.A.
gRNA2 sequence for CRISPR/Cas9 knock-in of 7×GFP11-HA into 5-HT2A isoform A: ttcgaggtgccttcgtcggt	Eurofins Genomics	N.A.
gRNA1 sequence for CRISPR/Cas9 knock-in of 7×GFP11-HA into 5-HT2A isoform D: tccttctggcgcaaacacgg	Eurofins Genomics	N.A.
gRNA2 sequence for CRISPR/Cas9 knock-in of 7×GFP11-HA into 5-HT2A isoform D: ctgaagacataattacgtgg	Eurofins Genomics	N.A.
gRNA1 sequence for CRISPR/Cas9 knock-in of 7×GFP11-HA into 5-HT2A isoform B, F and H: cgctatcggtctgtgacaga	Eurofins Genomics	N.A.
gRNA2 sequence for CRISPR/Cas9 knock-in of 7×GFP11-HA into 5-HT2A isoform B, F and H: ggaaaagccgctaattacag	Eurofins Genomics	N.A.
gRNA1 sequence for CRISPR/Cas9 knock-in of 7×GFP11-HA into 5-HT2B: aggcactcgtgctcgaatag	Eurofins Genomics	N.A.
gRNA2 sequence for CRISPR/Cas9 knock-in of 7×GFP11-HA into 5-HT2B: ttcagtttgcccggtttaac	Eurofins Genomics	N.A.
gRNA sequence for CRISPR/Cas9 knock-in of 1× and 7×GFP11-HA into 5-HT7: ggcgagggagagctttctct	Eurofins Genomics	N.A.
Forward primer for amplifying the left donor arm for CRISPR/Cas9 knock-in of 7×GFP11-HA into 5-HT1A: aattatgctAGCTAGAGGACCAGGACGAGC	Eurofins Genomics	N.A.
Reverse primer for amplifying the left donor arm for CRISPR/Cas9 knock-in of 7×GFP11-HA into 5-HT1A: ccatcgccgagctcccgcctGCGGTAGTG	Eurofins Genomics	N.A.
Forward primer for amplifying the right donor arm for CRISPR/Cas9 knock-in of 7×GFP11-HA into 5-HT1A: ccagattacgcttaaAGCGGaAAGCTCTAGATAGTGC	Eurofins Genomics	N.A.
Reverse primer for amplifying the right donor arm for CRISPR/Cas9 knock-in of 7×GFP11-HA into 5-HT1A: aattggcgCCGCTGGTCCGTTTAGCAGAAG	Eurofins Genomics	N.A.
Forward primer for amplifying the insert fragment for CRISPR/Cas9 knock-in of 7×GFP11-HA into 5-HT1A: agcgggaagctcggcgatggaggaagcg	Eurofins Genomics	N.A.
Reverse primer for amplifying the insert for CRISPR/Cas9 knock-in of 7×GFP11-HA into 5-HT1A: GCTTtCCGCTttaaagcgtaatctggaacatcgtatggg	Eurofins Genomics	N.A.

(Continued on next page)

Continued

REAGENT or RESOURCE	SOURCE	IDENTIFIER
Forward primer for amplifying the left donor arm for CRISPR/Cas9 knock-in of 7×GFP11-HA into 5-HT1B: taattgctagcgatgcggatgatgaagta	Eurofins Genomics	N.A.
Reverse primer for amplifying the left donor arm for CRISPR/Cas9 knock-in of 7×GFP11-HA into 5-HT1B: ctcatcgccgaaatttcgactgcgcgctc	Eurofins Genomics	N.A.
Forward primer for amplifying the right donor arm for CRISPR/Cas9 knock-in of 7×GFP11-HA into 5-HT1B: ccagattaccgcttaatgaagaataacgaggaccagattttg	Eurofins Genomics	N.A.
Reverse primer for amplifying the right donor arm for CRISPR/Cas9 knock-in of 7×GFP11-HA into 5-HT1B: ataattgcgccgatacatgtgcataccgaag	Eurofins Genomics	N.A.
Forward primer for amplifying the insert fragment for CRISPR/Cas9 knock-in of 7×GFP11-HA into 5-HT1B: gcgaaaatttcgcgatggaggaagcgg	Eurofins Genomics	N.A.
Reverse primer for amplifying the insert for CRISPR/Cas9 knock-in of 7×GFP11-HA into 5-HT1B: cctcgtattcttctaagcgtaactggaacatcgatggg	Eurofins Genomics	N.A.
Forward mutagenesis primer for silencing the PAM motif for CRISPR/Cas9 knock-in of 7×GFP11-HA into 5-HT1B: gccttcaagagAattctcttcgg	Eurofins Genomics	N.A.
Reverse mutagenesis primer for silencing the PAM motif for CRISPR/Cas9 knock-in of 7×GFP11-HA into 5-HT1B: ccgaagagaatTctcttgaagc	Eurofins Genomics	N.A.
Forward primer for amplifying the left donor arm for CRISPR/Cas9 knock-in of 7×GFP11-HA into 5-HT2A isoform D: aattgctagccattgtttggtaagccatg	Eurofins Genomics	N.A.
Reverse primer for amplifying the left donor arm for CRISPR/Cas9 knock-in of 7×GFP11-HA into 5-HT2A isoform D: CCATCGCCgtacctgtccattaggtttggatagccg	Eurofins Genomics	N.A.
Forward primer for amplifying the right donor arm for CRISPR/Cas9 knock-in of 7×GFP11-HA into 5-HT2A isoform D: GCTTAACTCTAGACtaataggaacacctgaagacataattacg	Eurofins Genomics	N.A.
Reverse primer for amplifying the right donor arm for CRISPR/Cas9 knock-in of 7×GFP11-HA into 5-HT2A isoform D: taattgcgCCgcttcaatggggacctctgag	Eurofins Genomics	N.A.
Forward primer for amplifying the insert fragment for CRISPR/Cas9 knock-in of 7×GFP11-HA into 5-HT2A isoform D: ctaattggacaggtacGGCGATGGAGGAAGCGGAG	Eurofins Genomics	N.A.
Reverse primer for amplifying the insert for CRISPR/Cas9 knock-in of 7×GFP11-HA into 5-HT2A isoform D: ggtgtttcttataGGTCTAGAGTTAAGCGTAATCTGGAAC	Eurofins Genomics	N.A.
Forward mutagenesis primer for silencing the PAM motif 1 for CRISPR/Cas9 knock-in of 7×GFP11-HA into 5-HT2A isoform D: gcaaacacggcgCctatcaaac	Eurofins Genomics	N.A.
Reverse mutagenesis primer for silencing the PAM motif 1 for CRISPR/Cas9 knock-in of 7×GFP11-HA into 5-HT2A isoform D: ggtttggatagGcgccgtgtttgc	Eurofins Genomics	N.A.

(Continued on next page)

Continued

REAGENT or RESOURCE	SOURCE	IDENTIFIER
Forward mutagenesis primer for silencing the PAM motif 2 for CRISPR/Cas9 knock-in of 7×GFP11-HA into 5- HT2A isoform D: gacataattacgtgggtgCtgactactgc	Eurofins Genomics	N.A.
Reverse mutagenesis primer for silencing the PAM motif 2 for CRISPR/Cas9 knock-in of 7×GFP11-HA into 5- HT2A isoform D: gcagtaagtcaGcaccacgtaattatgtc	Eurofins Genomics	N.A.
Forward primer for amplifying the left donor arm for CRISPR/Cas9 knock-in of 7×GFP11-HA into 5-HT2A isoform B, F and H: aattatgctagctgagtaacgggtatctgacag	Eurofins Genomics	N.A.
Reverse primer for amplifying the left donor arm for CRISPR/Cas9 knock-in of 7×GFP11-HA into 5- HT2A isoform B, F and H: ccatcgccgcactcgtctgtgactgtg	Eurofins Genomics	N.A.
Forward primer for amplifying the right donor arm for CRISPR/Cas9 knock-in of 7×GFP11-HA into 5- HT2A isoform B, F and H: cgcttaactctagacctaaccacgaggagcaccatc	Eurofins Genomics	N.A.
Reverse primer for amplifying the right donor arm for CRISPR/Cas9 knock-in of 7×GFP11-HA into 5- HT2A isoform B, F and H: tataattgcggccgctcgaaacgcttccttctgc	Eurofins Genomics	N.A.
Forward primer for amplifying the insert fragment for CRISPR/Cas9 knock-in of 7×GFP11-HA into 5- HT2A isoform B, F and H: cgacgagtcggcgatggaggaagcggag	Eurofins Genomics	N.A.
Reverse primer for amplifying the insert for CRISPR/Cas9 knock-in of 7×GFP11-HA into 5- HT2A isoform B, F and H: ctctgtgttcaggctagagttaagcgaatctggaac	Eurofins Genomics	N.A.
Forward mutagenesis primer for silencing the PAM motif 1 for CRISPR/Cas9 knock-in of 7×GFP11-HA into 5- HT2A isoform B, F and H: ctgtgacagaagCacgcggc	Eurofins Genomics	N.A.
Reverse mutagenesis primer for silencing the PAM motif 1 for CRISPR/Cas9 knock-in of 7×GFP11-HA into 5- HT2A isoform B, F and H: gccgcgtGcttctgtcacag	Eurofins Genomics	N.A.
Forward mutagenesis primer for silencing the PAM motif 2 for CRISPR/Cas9 knock-in of 7×GFP11-HA into 5- HT2A isoform B, F and H: cagaacaaaacggagtTcactgtaattagc	Eurofins Genomics	N.A.
Reverse mutagenesis primer for silencing the PAM motif 2 for CRISPR/Cas9 knock-in of 7×GFP11-HA into 5- HT2A isoform B, F and H: gctaattacagtgAactccgtttgtttctg	Eurofins Genomics	N.A.
Forward primer for amplifying the left donor arm for CRISPR/Cas9 knock-in of 7×GFP11-HA into 5-HT2B: AATATTCTAGATCCTCCGAGAAGGGC	Eurofins Genomics	N.A.
Reverse primer for amplifying the left donor arm for CRISPR/Cas9 knock-in of 7×GFP11-HA into 5- HT2B: ccatcgccgagTCTGCTCGGTCGCCAGGCAC	Eurofins Genomics	N.A.
Forward primer for amplifying the right donor arm for CRISPR/Cas9 knock-in of 7×GFP11-HA into 5- HT2B: gattacgcttaaTAACAGACGACCGTTAAACCGGGC	Eurofins Genomics	N.A.
Reverse primer for amplifying the right donor arm for CRISPR/Cas9 knock-in of 7×GFP11-HA into 5- HT2B: ataattgcggccGCAGCACATTCGAACTTTCATCCG	Eurofins Genomics	N.A.

(Continued on next page)

Continued

REAGENT or RESOURCE	SOURCE	IDENTIFIER
Forward primer for amplifying the insert fragment for CRISPR/Cas9 knock-in of 7×GFP11-HA into 5- HT2B: CCGAGCAGActcggcagtgagggaagcg	Eurofins Genomics	N.A.
Reverse primer for amplifying the insert for CRISPR/Cas9 knock-in of 7×GFP11-HA into 5- HT2B: ttaaaGGTACCCGGTTAACGGTCGCTCTG	Eurofins Genomics	N.A.
Forward mutagenesis primer for silencing the PAM motif 1 for CRISPR/Cas9 knock-in of 7×GFP11-HA into 5- HT2B: GTCCTGCTGTGTCGCTATTCGAGC	Eurofins Genomics	N.A.
Reverse mutagenesis primer for silencing the PAM motif 1 for CRISPR/Cas9 knock-in of 7×GFP11-HA into 5- HT2B: GCTCGAATAGCGACACAGCAGGAC	Eurofins Genomics	N.A.
Forward primer for amplifying the left donor arm for CRISPR/Cas9 knock-in of 7×GFP11-HA into 5-HT7: aatagtagcactgtagtgaggcaatgccc	Eurofins Genomics	N.A.
Reverse primer for amplifying the left donor arm for CRISPR/Cas9 knock-in of 7×GFP11-HA into 5- HT7: ctccatgccgagaagctctccctgccccgtg	Eurofins Genomics	N.A.
Forward primer for amplifying the right donor arm for CRISPR/Cas9 knock-in of 7×GFP11-HA into 5- HT7: ccagattacgcttaactctagaccatccagaggacccc	Eurofins Genomics	N.A.
Reverse primer for amplifying the right donor arm for CRISPR/Cas9 knock-in of 7×GFP11-HA into 5- HT7: taattgcccgcagggggctgggtatttac	Eurofins Genomics	N.A.
Forward primer for amplifying the insert fragment for CRISPR/Cas9 knock-in of 7×GFP11-HA into 5- HT7: gggagagctttctcggcagtgagggaagcg	Eurofins Genomics	N.A.
Reverse primer for amplifying the insert for CRISPR/Cas9 knock-in of 7×GFP11-HA into 5- HT7: ggtctagagttaagcgtaatctggaacatcgtatggtaactagtaatgccagctgccc	Eurofins Genomics	N.A.

Recombinant DNA

pTwist Amp	Twist Bioscience HQ, CA	
pTwist Amp_d5-HT7R-7xsfGFP11-HA-HDR-donor	This study	Addgene # 221818
pTwist Amp_d5-HT7R-sfGFP11-HA-CRISPR-HDR-donor	This study	Addgene # 221819
pdU6-2_sgRNA-d5-HT1AR	This study	Addgene # 221820
pdU6-2_sgRNA1-d5-HT1BR	This study	Addgene # 221821
pdU6-2_sgRNA2-5-HT1BR	This study	Addgene # 221822
pdU6-2_sgRNA1-5-HT2AR-isoformD	This study	Addgene # 221823
pdU6-2_sgRNA2-5-HT2AR-isoformD	This study	Addgene # 221824
pdU6-2_sgRNA1-5-HT2AR-isoformBFH	This study	Addgene # 221825
pdU6-2_sgRNA2-5-HT2AR-isoformBFH	This study	Addgene # 221826
pdU6-2_sgRNA1-d5-HT2BR	This study	Addgene # 221827
pdU6-2_sgRNA2-d5-HT2BR	This study	Addgene # 221828
pdU6-2_sgRNA-d5-HT7R	This study	Addgene # 221829
pdU6-2_sgRNA1-for-dSERT	This study	Addgene # 221830
pdU6-2_sgRNA2-for-dSERT	This study	Addgene # 221831
pTwist Amp_d5-HT1AR-7xsfGFP11-HA-HDR-donor	This study	Addgene # 221832
pTwist Amp_d5-HT2BR-7xsfGFP11-HA-HDR-donor	This study	Addgene # 221833

(Continued on next page)

Continued

REAGENT or RESOURCE	SOURCE	IDENTIFIER
13xLexAop2 IVS sfGFP1-10	This study	Addgene # 221834
pTwist Amp_2xFlag-dSERT-HDR-donor-HDR	This study	Addgene # 221835
pACUH 5-HT7R-7xGFP11-HA	This study	Addgene # 221836
pTwist Amp_d5-HT1BR-7xsfGFP11-HA-HDR-donor	This study	Addgene # 221837
pTwist Amp_d5-HT2AR(isoformD)-7xsfGFP11-HA-HDR-donor	This study	Addgene # 221838
pTwist Amp_d5-HT2AR(isoformBFH)-7xsfGFP11-HA-HDR-donor	This study	Addgene # 221839
pACUH 5-HT2BR-7xGFP11-HA	This study	Addgene # 221840

Software and algorithms

ImageJ	https://imagej.net/ij/
--------	---

Other

Glass slides	VWR	16004-422
Glass coverslips, 25×25 mm	VWR	48366-089
Glass coverslips, 18×18 mm	VWR	48366-045

EXPERIMENTAL MODEL AND STUDY PARTICIPANT DETAILS

In this study we have employed female *Drosophila melanogaster* as a model system. Male *Drosophila* also undergoes critical period plasticity.²⁷ The specific genotypes of the flies in the figures can be found in Table 1. Information about fly rearing, maintenance, specific experimental conditions can be found in the relevant sections below.

METHOD DETAILS**Fly rearing and maintenance**

All *Drosophila* lines were raised in sparse cultures on cornmeal, yeast, dextrose medium¹⁰³ at 25°C in a 12hour light/dark cycle unless otherwise noted. The fly lines used in this study can be found in Tables 1 and S1. We used female flies for our studies, except where specifically mentioned. Flies used in the CO₂ and air exposure experiments were raised at 25°C until the 4-day old pupae stage and at 23°C until they were sacrificed.

Selective Serotonin Reuptake Inhibitor (SSRI) Treatment

For treatments with SSRI, fluoxetine hydrochloride (56296–78-7) and escitalopram oxalate (219861–08-2) were purchased from Sigma Aldrich. 3mM SSRI containing fly food was made fresh daily as described in Bonanno and Krantz et al., 2023.¹⁰⁴ Flies were grown until pupal stage in the same growing media and bottle until 4day old pupae, at which point they were separated into fresh vials of food. On day 5 after eclosion, flies were transferred into food vials containing 3mM fluoxetine or escitalopram and incubated at 25°C overnight. On day 6, flies were transferred into separate food vials containing either SSRI and exposed to either CO₂ or air for 4 days at 23°C.

Odor exposure

We employed previously established odor exposure protocol to induce critical period plasticity in the flies^{21,23} Briefly, 4-day old pupae of relevant genotype were collected into separate vials based on odor-exposure. A fine mesh cheesecloth was secured at the opening of the fly vial to ensure free gaseous exchange. Fly vials were placed in either a temperature-controlled CO₂ or regular incubator at 23°C on 12-hour light/dark cycles. Eclosed flies were transferred into clean vials 18-21 hours after the start of odor exposure until day 5 post eclosion when they were collected for dissection and immunohistochemistry. For each of the odor exposure experiments, pupae for all the genotypes including control lines for the Gal4 and RNAi and Canton-S (wild-type) were collected on the same day and odor exposure started at the same time. Pupae of the same genotype were collected from the same stock bottle and separated into odor exposed (CO₂) and control (air) vials to ensure consistency in food composition, availability, and conditions. During odor exposure both male and female flies of a specific genotype were present in each vial. Only female flies were collected after cold anesthetizing the flies at the end of the experiment right before dissection.

Plasmid preparation for CRISPR/Cas9 knock-in

The GFP₁₁-HA was synthesized *de novo* by Twist Bioscience, CA and the coding sequence was knocked-in the fly genome using CRISPR/Cas9 via homology-directed repair (HDR). Two plasmid DNAs were prepared for each knock-in preparation: the guide RNA (gRNA) plasmid and the donor plasmid. The gRNA plasmid was prepared following a previously established protocol.⁶⁵ Briefly, a pair of 24 nucleotide oligos were commercially synthesized as for normal unsalted primers (Eurofins Genomics). For each oligo, the first 4 nucleotides (TTCG for the sense

strand and AAAC for the antisense strand) at the 5' end formed the overhanging sequence after reannealing. These overhanging nucleotides were compatible with the Bbs I digestion sites of the plasmid dU6-2 (See [Data S1](#) for the full sequence), while the remaining 20 nucleotides carried the sense or antisense strand of the target sequence for the insertion site in the genome. The 20-nt target sequences (sense) were identified close to the C-terminus of the 5-HTR coding region using an online tool FlyCRISPR⁶⁶ for 5-HT receptor (5-HTR) genes, as listed in Table. The backbone for gRNA expression, dU6-2, was digested with Bbs I and ligated with the reannealed 24-nt oligo pairs with T4 DNA ligase. To prepare the donor plasmid, approximately one kilo basepair of DNA upstream of the insertion site was PCR'd as the left arm for homology directed repair (HDR). Similarly, about one kilo basepair of 5-HTR DNA in the downstream of the insertion site was PCR'd as the right arm for HDR. The encoding sequence of GFP₁₁-HA was then inserted in between both arms via overlap extension PCRs. The resultant PCR product was then inserted into pTwist Amp plasmid (High copy, Twist Bioscience HQ, CA) via restriction digestion and ligation with Rapid DNA Ligation Kit (Thermo Fisher Scientific, Cat. # K1422). For both plasmids, the ligation mixture was then used for transformation of *E. coli* strain DH5 α (Thermo Fisher Scientific, Cat. # EC0112). Single colonies of DH5 α were used for inoculation of 10 mL mini cultures with LB medium supplemented with 100 μ g/mL ampicillin (Thermo Fisher Scientific, Cat. # J60977.06). After overnight incubation with vigorous shaking, plasmid DNA was prepared from the culture using the NucleoSpin Plasmid Mini kit (MACHEREY-NAGEL, Cat. # 740588.250). The purified DNA was digested with restriction enzymes for quality control and subject to sequencing analysis for verification.

Coding sequences of guide RNA (gRNA) spacers for CRISPR/Cas9 knock-in of GFP11-HA in 5-HTR genes

Receptor name	Open-reading frame	Gene ID	gRNA sequence (with thymine)
5-HT1A	CG16720	37196	gaccagtccactaccgcagc
5-HT1B	CG15113	37191	aatttcgacgggcttcaag (gRNA1) gaaaatttgattcaactga (gRNA2)
5-HT2A	CG1056	40575	catattcaatcgcacgttcc (gRNA1 for isoform A) ttcgaggtgccttcgtcggt (gRNA2 for isoform A) tccttctggcgcaaacacgg (gRNA1 for isoform D) ctgaagacataattacgtgg (gRNA2 for isoform D) cgctatcggtctgtgacaga (gRNA1 for isoforms B, F and H) ggaaaagccgctaattacag (gRNA2 for isoforms B, F and H)
5-HT2B	CG42796	41017	aggcactcgtgctcgaatag (gRNA1) ttcagttgcccgtttaac (gRNA2)
5-HT7	CG12073	43669	ggcgagggagagcttctct

Extraction of genomic DNA

To extract the genomic DNA from adult flies or larvae for generating PCR templates, 2 flies were smashed in 50 μ L of Squishing buffer (10 mM TrisCl with pH 8.2, 1 mM EDTA, 25 mM NaCl and 200 μ g/mL freshly added Proteinase K) with a 200- μ L pipette tip in a PCR tube. The mixture was incubated at 50°C for 30 minutes before inactivated at 95°C for 5 minutes. After it cooled down, 0.5 to 1 μ L of the supernatant was used for the PCR template.

Generation of fly lines

To generate the 5-HTR-GFP₁₁-HA transgenic lines, the gRNA plasmid and the donor plasmid was co-injected with a 1:1 mass ratio into fly embryos by Rainbow Transgenic Flies, Inc. (California, USA). The genotype of the embryos was *y,sc,v; {nos-Cas9}attP2* for 5-HT1A and -1B, or *y,sc,v; {nos-Cas9}attP40/CyO* for 5-HT2A, -2B and -7. Depending on which chromosome the 5-HTR gene is on, the candidate flies were individually balanced with *Cyo* (for 5-HT1A and -1B) by crossing with *w1118*; *Cyo/Sco*, or *Tm6b, Tb, Hu* (for 5-HT2A, -2B and -7) by crossing with *w1118*; *Tm6b, Tb, Hu/MKRS*. The *nos-Cas9* transgene was finally removed by selecting progeny against red eyes.

Screening for successful knock-in was performed using PCR with a pair of primers targeting respectively the upstream and the downstream of the inserted sequence in the genomic DNA extracted from the candidate transformants. For PCR template, the genomic DNA was extracted from the daughter flies of individual injected embryos. Immunostaining against the HA-tag was used as the second step of verification.

Immunostaining and confocal imaging

All immunohistochemistry was performed using a standard protocol as previously described unless otherwise noted.^{44,103} For volume measurement experiments, the brains were incubated in the mounting medium for 1 hour before imaging to allow equilibration.¹⁰⁵ For imaging HA and split-GFP, the immunohistochemistry protocol was slightly modified. Briefly, the flies were anesthetized in a glass vial on ice for 1 min. The brains were dissected in PBS and fixed in 4% formaldehyde (37%, diluted in PBS) at room temperature. After three times of washing each for 15 min with 0.2% PBST, i.e., PBS supplemented with 0.2% (v/v) Triton X-100 (Thermo Fisher Scientific, Cat. # A16046.AE), the brains were blocked in 10% normal goat serum (NGS; Thermo Fisher Scientific, Cat. # PCN5000) at room temperature for 1 - 2 hours. Next, the brains were incubated with primary antibodies diluted in 0.2% PBST supplemented with 5% NGS at 4° for 3 to 4 days. Then the brains were washed with 0.2% PBST three times each for 15 min, and subject to incubation with secondary antibodies diluted in 0.2% PBST supplemented with 5%

NGS in a dark environment at 4° for 1 day. Table 2 lists all the antibodies used in this study. After washing with 0.2% PBST four times each for 10 min, the brains were mounted on glass slides (VWR, Cat. # 16004-422) with VECTASHIELD Antifade Mounting Medium (Vector Laboratories, Cat. # H-1000-10) and covered with glass coverslips (VWR, Cat. # 48366-089). To prevent the brains from being smashed, two smaller coverslips (VWR, Cat. # 48366-045) were placed as spacers between the glass slide and the covering coverslip with one on each side. The coverslips were fixed with a few drops of nail polish on the edge. All samples were scanned with a confocal microscope in the institution imaging facility: ZEISS LSM980, ZEISS LSM 710 or PerkinElmer Spinning disk. Brains used in the same experiment were imaged on the same day, under the same microscope and image acquisition settings. For validation of the VMAT-RNAi, brains were immunolabeled for GFP and 5-HT as described in Coates et al., 2017³⁸ and imaged with an Olympus Fluoview 1000.

QUANTIFICATION AND STATISTICAL ANALYSIS

Image analysis

For measuring the volume of the glomerulus, we performed image segmentation by specifying the borders of the specific glomerulus across the Z-stack of the confocal image based on n-cad staining using the segmentation plugin in ImageJ.¹ The volume of the selected glomeruli was obtained by 3-D analysis of the segmented image using the MorphoLibJ¹⁰⁶ plugin in ImageJ. Absolute volume is computed in this plugin by multiplying the number of voxels comprising the selection with the volume of individual voxel. The resultant glomeruli volumes were found to be consistent with those previously reported.^{21,27} Approximately 15 samples were analyzed for each genotype, age, or odor exposure unless otherwise noted. An unpaired Student's t-test was used to compare the difference in glomerular volumes of air and CO₂ exposed flies or fluorescence intensity between sexes or across fly of different ages. The p-values are indicated as * for $p < 0.05$ and as N.S for non-significance ($p > 0.05$) unless otherwise noted in the figure legends. All violin plots were created using code generated by Bechtold, Bastian 2016 (<https://github.com/bastibe/Violinplot-Matlab>) on Github.

To measure the efficacy of the VMAT-RNAi in Figure 1, we compared the intensity of 5-HT immunolabeling between the CSDns and 5-HT+ cells not expressed by R60F02-GAL4. Max projection Z-stacks were generated from confocal images and ROIs were manually drawn around the cell bodies of the CSDns and 5-HT+ neurons within the SEZ (control cells) at similar depths using the "freehand selections" tool in ImageJ. Fluorescence intensity measurements were acquired from cells in both hemispheres to account for the two CSDns per brain. These measurements were then converted into a ratio of 5-HT fluorescence = CSDn fluorescence/Control cell fluorescence. Ratios per CSDn were averaged across genotypes and compared using an unpaired Mann-Whitney test.

The fluorescence intensity measurements in Figure S2 were normalized for each glomerulus against the fluorescence intensity of the VL1 glomerulus. This was done to show the fold-difference in 5-HT2B expression in the selected glomeruli in comparison to a glomerulus of average 5-HT2B expression. The fluorescence intensity measurements reported in Figure 6B were obtained using previously described methodology in ImageJ.¹⁰⁷ Briefly, the corrected total cell fluorescence for each sample reported was calculated by subtracting the product of the area of the AL and mean background fluorescence of the brain outside the AL from the integrated density of the AL.